R-08-138

Emplacement mechanisms and structural influences of a younger granite intrusion into older wall rocks – a principal study with application to the Götemar and Uthammar granites

Site-descriptive modelling SDM-Site Laxemar

Alexander R Cruden
Department of Geology, University of Toronto

December 2008

Svensk Kärnbränslehantering AB
Swedish Nuclear Fuel
and Waste Management Co

Box 250, SE-101 24 Stockholm
Phone +46 8 459 84 00

ISSN 1402-3091
SKB Rapport R-08-138

Emplacement mechanisms and structural influences of a younger granite intrusion into older wall rocks – a principal study with application to the Götemar and Uthammar granites

Site-descriptive modelling SDM-Site Laxemar

Alexander R Cruden
Department of Geology, University of Toronto

December 2008

Abstract

The c. 1.80 Ga old bedrock in the Laxemar-Simpevarp area, which is the focus of the site investigation at Oskarshamn, is dominated by intrusive rocks belonging to the c. 1.86–1.65 Ga Transscandinavian Igneous Belt (TIB). However, the site investigation area is situated in between two c. 1.45 Ga old anorogenic granites, the Götemar granite in the north and the Uthammar granite in the south. This study evaluates the emplacement mechanism of these intrusions and their structural influence on the older bedrock. Field observations and structural measurments indicate that both the Götemar and the Uthammar granites are discordant and have not imposed any significant ductile deformation on their wall-rocks. The apparent conformity of geological contacts and fabrics in the wall rocks and the southern margin of the Götemar granite is coincidental and inherited from the pattern of Svecokarelian deformation of the TIB. However, interpretation of regional aeromagnetic data suggests that the granites occur within a broad, NNE-SSW trending linear belt, pointing to deep seated tectonic control on their generation, ascent and emplacement. Thermochronology indicates that the granites were emplaced at depths between 4 and 8 km into brittle wall rocks.

The 3-D shape of the Götemar and Uthammar plutons has been investigated by 2.75D forward modelling of the residual gravity anomalies due to both granites. Both granites are associated with strong residual gravity anomalies of up to –10 mgal. Constraints on the geometry of the plutons at the surface are provided from surface geology maps and several deep boreholes located on or close to the model profiles. A further variable in the gravity modelling is introduced by either allowing the upper contact of the plutons to assume the most suitable orientation to produce the best fit between the modelled and observed gravity ("unconstrained models") or by forcing the near surface orientation of the contacts to be vertical ("constrained models"). The unconstrained model profiles for both plutons are characterized by gently outward dipping upper contacts to depths ~1 km, gently inward dipping lower contacts and a thin, centrally located root extending to depths of 5 to 10 km. However, this geometry is not supported by available boreholes, which do not penetrate the upper contact of the Götemar pluton as predicted by the models. The constrained models are consistent with borehole data. They characterize the plutons as having vertical contacts in the upper 500 to 1,000 m, a 1,000 to 1,500 m thick mid-level body with outward dipping upper and horizontal and lower contacts, respectively, and broad roots extending to depths of ~4 km.

Preliminary observations and gravity modelling results indicate that the Götemar and Uthammar granites are discordant plutons with geometries most consistent with punched laccoliths, with some modification due to floor subsidence due to root development. Their vertical and lateral dimensions fall in the upper range for laccoliths and lower range for plutons as defined by recent data compilations. Their emplacement required elastic bending and eventual failure of roof rocks that was likely accompanied by reactivation of pre-existing fractures and shear zones and possibly the creation of new brittle fractures. Cooling and crystallization of the granites resulted in thermal resetting of the wall rocks and the establishment of a transient hydrothermal system, now recorded by fracture filling mineral assemblages.

Sammanfattning

Berggrunden i Laxemar-Simpevarpsområdet, som är fokus för platsundersökningen i Oskarsham, domineras av ca 1 800 miljoner år gamla intrusiva bergarter som tillhör det 1 860–1 650 miljoner år gamla Transskandinaviska magmatiska bältet (TMB). Platsundersökningsområdet är dock beläget mellan två ca 1 450 miljoner år gamla anorogena graniter, Götemargraniten i norr och Uthammargraniten i söder. Denna studie behandlar intrusionsmekanismen av dessa graniter och dess strukturella påverkan på den äldre berggrunden. Fältobservationer och strukturella mätningar indikerar att både Götemar- och Uthammargraniten är diskordanta och har inte orsakat någon plastisk deformation i sidoberget. Den skenbara parallelliteten mellan bergartskontakter och strukturer i sidoberget och Götemargranitens södra kontakt är av tillfällig natur. Det strukturella mönstret i TMB-bergarterna är ett resultat av deformationer i slutskedet av den svekokarelska orogenesen. En tolkning av regionala magnetiska anomalidata tyder istället på att graniterna förekommer inom ett brett NNO-SSV-ligt linjärt bälte vilket indikerar en djupliggande tektonisk kontroll av de ursprungliga magmornas bildning, uppåtstigande och slutligt läge i jordskorpan. Termokronologiska beräkningar indikerar att graniterna intruderade på ett djup mellan 4 och 8 km i ett sprött sidoberg.

Götemar- och Uthammargraniternas tredimensionella geometri har undersökts med hjälp av 2.75D modellering av de båda graniternas residuala tyngdkraftsanomalier. Både Götemar- och Uthammargraniten är associerad med kraftiga residuala tyngdkraftsanomalier på upp till –10 mgal. Graniternas geometri på ytan och i den allra översta delen av jordskorpan baseras på befintliga berggrundskartor och information från de borrhål som förekommer på eller i närheten av de modellerade profilerna. En ytterligare variabel i tyngdkraftsmodelleringen är att man antingen tillåter graniternas övre kontakt anta den bästa anpassningen mellan den modellerade och observerade tyngdkraften (”unconstrained models”), eller att man antar att kontakterna i den allra översta delen av jordskorpan är vertikala (”constrained models”). Profilerna i ”unconstrained models” karakteriseras av att graniternas övre kontakter stupar flackt utåt till ett djup a ca 1 km, flackt inåtstupande nedre kontakter och en tunn centralt lokaliserad rot som sträcker sig ner till ett djup av 5 till 10 km. Dessa modeller stöds emellertid inte av befintliga borrhål eftersom dessa inte nått graniternas övre kontakt, vilket de skulle ha gjort enligt ”unconstrained” modellering. ”Constrained” modellering överensstämmer dock med borrhålsdata. Enligt denna har graniterna vertikala kontakter ner till 500 till 1 000 m, en 1 000 till 1 500 m tjock central kropp med utåtstupande övre kontakter och horisontella nedre kontakter samt en bred rot som sträcker sig ner till ett djup av ca 4 km.

Preliminära observationer och resultaten av tyngdkraftsmodelleringen indikerar att Götemar-och Uthammargraniterna är diskordanta och med 3D geometrier som bäst överensstämmer med en lakkolit, dock kortare och tjockare (”punched laccolith”) än typfallet, med vissa modifieringar beroende på nersjunkning av den nedre delen beroende på utvecklingen av kropparnas rot. Graniternas vertikala och laterala dimensioner faller inom den övre gränsen för lakkoliter och den nedre gränsen för plutoner enligt definitioner baserade på sammanställningar av nya data. Intrusionen av graniterna innebar en elastisk böjning av och eventuella brott i de ovanliggande bergarterna. Detta kan ha åtföljts av reaktivering av existerande sprickor och skjuvzoner samt möjligen också bildning av nya sprickor. Avkylningen och kristallisationen av graniterna resulterade i en termisk påverkan på sidoberget och bildandet av ett hydrotermalt system då sprickfyllnader relaterade till graniterna observerats i Laxemar.

Contents

1 Introduction

The c. 1.80 Ga old bedrock in the Laxemar-Simpevarp area, which is the focus of the site investigation at Oskarshamn, is dominated by intrusive rocks belonging to the c. 1.86–1.65 Ga Transscandinavian Igneous Belt (TIB). However, the site investigation area is situated in between two c. 1.45 Ga old granites, the Götemar granite in the north and the Uthammar granite in the south. The question of a possible structural influence on the older bedrock during the emplacement of these granites has been raised during the ongoing site investigation.

Geological mapping and rock domain modelling constrained by boreholes, potential field and seismic reflection data indicate that at the surface the contacts between the major lithological domains within the Laxemar-Simpevarp area are more or less conformable to the southern contact of the Götemar granite, but not to the northern contact to the Uthammar granite. This conformable relationship at the surface has traditionally been regarded as conspicuous and has raised the question as to whether it may have been caused by emplacement of the Götemar granite. However, rock domain modelling shows that a similar conformable relationship does not exist at depth /Wahlgren et al. 2008/. Furthermore, such a relationship requires that the older rocks behaved in a ductile manner during the emplacement of the younger granite. Available $^{40}Ar/^{39}Ar$ biotite data indicate that the temperature in the bedrock in the Laxemar-Simpevarp area passed below a temperature of c. 300°C at c. 1.5 Ga /Page et al. 2007, Söderlund et al. 2008/, and hence below the expected ductile deformation field, before the time of emplacement of the younger granites at c. 1.45 Ga.

An alternative explanation is that the conformable relationship is coincidental and that the present configuration of the older rocks is related to the original intrusion of the c. 1.80 Ga TIB rocks several hundreds of million of years prior to emplacement of the Götemar and Uthammar granites and subsequent sinistral displacements along NE-trending ductile shear zones. The latter are interpreted to predate, and are therefore unrelated to the Götemar granite.

1.1 Objective and scope

The objective of the present study is to evaluate the emplacement mechanisms of the Götemar and Uthammar granites and to thereby determine their structural and thermal influence on the intervening wall rocks in the Laxemar-Simpevarp area. The scope of the study is to:

1) provide a critical assessment of all relevant geological and geophysical data pertaining to the structure of the Götemar and Uthammar granites and their wall rocks;
2) develop a structural interpretation of the bedrock geology located between the Götemar and Uthammar granites, with particular emphasis on delineating structural features that formed prior to, during and after their emplacement; and
3) to provide general recommendations and conclusions regarding the structural influences of younger granites on older Proterozoic crystalline bedrock in south and central Sweden, with particular emphasis on implications for nuclear waste repository engineering.

In the context of the scope and objectives of the study, a state-of-the-art review of granite emplacement studies is also provided, with specific examples from the Svecokarelian (Svecofennian) orogen of southern Sweden.

2 Review of granite emplacement studies

The modes of ascent and emplacement of granitic intrusions have been outstanding problems in geology since the work of James Hutton in the 18th century. Modern studies of the problem distinguish between the processes of magma generation, ascent and emplacement, and this review focuses on the latter two of these. Evaluation of the relative timing and mechanism of emplacement of a granite intrusion requires detailed information on its three dimensional shape and its internal and external structure. Hence, a combined approach incorporating modelling and interpretation of geophysical data (gravity, magnetic, seismic) and geological mapping is recommended for the study of pluton emplacement studies /Cruden et al. 1999a, Ameglio and Vigneresse 1999/. The following review and the investigation of the Götemar and Uthammar granites uses such an approach.

The following terminology is employed for different classes of igneous intrusion in this report:

Pluton. Historical Usage: *a body of rock formed by metasomatism. …The term originally signified only deep seated or plutonic bodies of granitoid texture* /Corry 1988/. Modern Usage 1: An informal term for *an igneous intrusion whose form is irregular such that it cannot be classified as a laccolith, dyke, sill or other recognised body* (more correctly termed *chonolith*; /Corry 1988/). Modern Usage 2 (used in this report): *a granitic body of the order 1–200 km^2 in outcrop, built from one or more pulses of magma yet clearly circumscribed by its country rock envelope* /Pitcher 1993/.

Batholith. An informal term for *a large, generally discordant plutonic mass > 100 km^2 in surface exposure with no known floor* /Corry 1988/. Modern researchers consider batholiths to comprise *an array (or collection) of individual plutons* /Pitcher 1993/.

Dyke. An informal term for *a tabular igneous intrusion that cuts across the bedding or foliation of the country rock* /Corry 1988/.

Sill. An informal term for *a tabular igneous intrusion that parallels the planar structure of the surrounding rock* /Corry 1988/.

Laccolith. *A concordant igneous intrusion with a known or assumed flat floor and a postulated dykelike feeder commonly thought to be beneath its thickest part. It is generally plano-convex in form and roughly circular in plan, less than 10 km in diameter, and from a few m to several hundred m in thickness* /Corry 1988/.

Lopolith. *A large, concordant, typically layered igneous intrusion, of plano convex or lenticular shape, that is sunken in its central part owing to sagging of the underlying country rock* /Corry 1988/.

2.1 Shapes, external and internal structures of granitic plutons

Historically, granitic plutons have been viewed as areally extensive intrusions with steep sides that continue to great depth in the crust /e.g. Buddington 1959, Paterson et al. 1996, Miller and Paterson 1999/. Such a perception is largely a function of a sampling bias; erosion of a several kilometre thick, tabular body in an area of low to modest relief will tend to favour exposure of steep pluton walls. Preservation of roofs and dissection through floors is only likely in areas where relief is greater than or equal to pluton thicknesses. This sampling problem is further compounded because uplift and erosion levels tend to stabilise close to the roofs of plutons /Leake and Cobbing 1993, McCaffrey and Petford 1997/. However, a sufficient body of field- and geophysics-based data is now available in the literature to make several generalisations on the three-dimensional form of the majority of granitic plutons.

Because erosion is usually insufficient to expose both the floors and roofs of the majority of plutons, gravity, magnetic or seismic data must be employed in order to estimate their thicknesses /e.g. Bott and Smithson 1967, Sweeny 1976, Lynn et al. 1981, Brun et al. 1990, Evans et al. 1994, Vigneresse 1995, Ameglio and Vigneresse 1999, Cruden et al. 1999a, Roy and Clowes 2000, Taylor 2007/. Less frequently, tilted sections /e.g. John and Mukasa 1990, Miller et al. 1990/, deep erosional dissection /e.g. Hamilton and Myers 1967, Myers 1975, Le Fort 1981, Scaillet et al. 1995, Rosenberg et al. 1995, Skarmeta and Castellini 1997, Grocott et al. 1999/ or analysis of structural patterns /e.g. Brun and Pons 1981, Cruden et al. 1999b, Saint-Blanquat et al. 2001, Stevenson et al. 2007ab/ provide direct or projected estimates of pluton thicknesses. In these cases both the roof and floor are often observed, whereas geophysical data usually only provides information on thickness from a sub-roof erosion level to the pluton floor. Despite this limitation, geophysical estimates of pluton thickness are similar in magnitude to field observations, as discussed in Section 2.1.7. Key observations on the nature of typical pluton structure are reviewed briefly in the following sections, with specific reference to two case studies in central Sweden (Figure 2-1 and Figure 2-2).

2.1.1 Ljugaren Granite, central Sweden

The c. 1.70 Ga semi-circular Ljugaren granite intrudes amphibolite facies gneisses of the Svecokarelian orogen (Figure 2-1). Its structural characteristics are representative of a post-tectonic mesozonal pluton /Buddington 1959/ emplaced into medium- to high-grade meta-intrusive and supracrustal rocks. Such plutons have frequently been interpreted to be igneous diapirs /e.g. Sylvester 1964, Holder 1979, Bateman 1984, Castro 1986, Courrioux 1987/. The Ljugaren granite is bound to the west by the East Siljan fault, which is a Svecokarelian structure reactivated during formation of the Devonian Siljan Ring impact structure /Cruden and Aaro 1992/. Foliations and lithological contacts in gneisses and granites surrounding the pluton are bent into conformity with its steeply inward dipping contacts. Foliation trajectories are markedly asymmetric and suggest that the gneisses were displaced laterally to the east during emplacement. The granite itself is homogeneous, displays igneous microstructure and contains a weakly defined foliation concentric to its east half and a down-dip lineation where observed (Figure 2-1). The Ljugaren granite is associated with a residual gravity anomaly (> –6 mgal), centred on the west central part of the pluton within the East Siljan fault, which decreases outwards towards the margins /Cruden and Aaro 1992/. Model gravity profiles indicate that the bulk of the pluton is tabular and < 3 km thick with a deeper (~6 km) root on its west side (Figure 2-1). Although the pluton roof is not exposed, regional considerations suggest that the granite spread beneath a cover sequence of syngenetic volcanics (Dala Series). Examination of the structural pattern in combination with the gravity data suggests that the ductile wall rocks must have been displaced downwards as well as outwards during emplacement of the granite and that movement of magma was from west to east, emanating from a conduit coincident with the East Siljan fault /Cruden 1998/. Similar examples of asymmetric filling of a sill-like intrusion accompanied by ductile wall rock deflection have been documented in California, western and central Canada /e.g. Cruden and Launeau 1994, Brown and McLelland 2000, de Saint-Blanquat et al. 2001/.

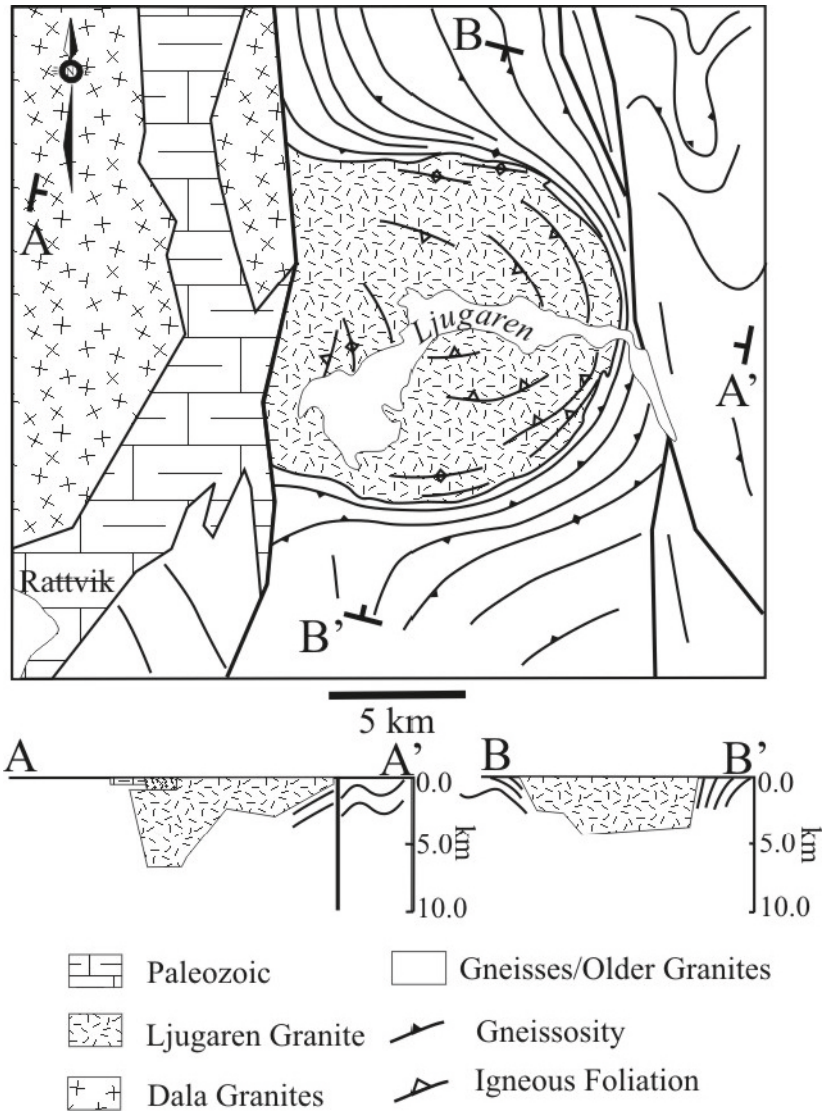

Figure 2-1. *Ljugaren granite, central Sweden /after Cruden and Aaro 1992/. Cross sections A-A' and B-B' are based on 2.5 D forward models of residual gravity anomalies, combined with field mapping data. Paleozoic sedimentary and Proterozoic igneous rocks west of the Ljugaren granite are exposed in the Devonian Siljan Ring impact structure, which has modified the western margin of the pluton.*

2.1.2 Gåsborn Granite, central Sweden

A second example of a combined geophysical/structural analysis of a pluton is provided by the c. 1.80 Ga Gåsborn granite in the Svecokarelian orogen (Figure 2-2), which has also been interpreted as a diapiric intrusion /Björk 1986/. Emplaced into greenschist facies metasedimentary and metavolcanic rocks and associated with a narrow (0 to 100 m) contact metamorphic aureole, the pluton is representative of a syn- to post-tectonic, epizonal to mesozonal intrusion /Buddington 1959/. Although the granite is exposed in an equant, almost spherical outcrop pattern, aeromagnetic and gravity data indicate that it is markedly asymmetric in cross section /Cruden et al. 1999a/. Gravity models suggest that the Gåsborn granite consists of an up to 3 km deep, NW-SE trending root zone that overlies the trace of a major structural break in the wall rocks, a ~2 km thick mass west of the root, and a < 1 km thick flap east of the root (Figure 2-2). The western margin of the pluton cuts across and apparently deflects and overturns the western limb of a tight, upright regional syncline. A stratigraphic contact between metavolcanic units on the eastern side is deflected and truncated by the granite, but also dips under the pluton, steepening as it approaches the contact. The modest amount of wall-rock deflection on the western margin can be accounted for by regional post-emplacement transpressive strains that

were accumulated during cooling of the pluton and development of a NW-SE trending subvertical tectonic foliation within the granite. The more dramatic deflection of stratigraphy adjacent to the eastern margin and its pluton-side-down deflection cannot be accounted for by regional post-emplacement strains and has been attributed to the combined effects of lateral spreading of the pluton from the root zone and associated downfolding of wall rocks /Cruden et al. 1999a/. The Gåsborn granite is syntectonic in the sense that magma transport was channelled along a major regional structure and emplacement and subsequent syn-cooling deformation occurred in a regime of regional transpression. However, space-creation and the resulting 3-D form of the pluton appear to have been controlled by internal processes and variations in wall rock mechanical properties. This can be understood in terms of rates, in which ductile Svecokarelian strains were accumulated over a time frame of millions of years, far longer than the time frame for pluton emplacement and crystallisation /viz. Paterson and Tobisch 1992/. The structure of the Gåsborn granite and its relationship to regional ductile shear zones is similar to plutons in other transpressive orogens, such as the New England Appalachians /Brown and Solar 1998/.

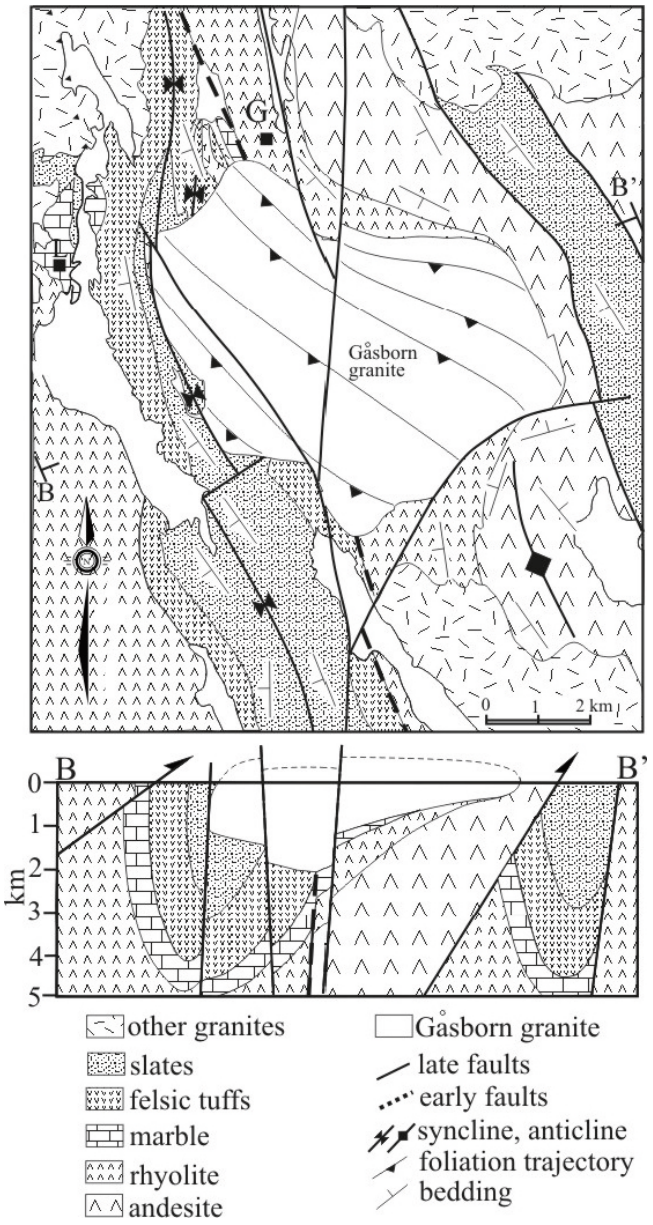

Figure 2-2. *Gåsborn granite, central Sweden /after Björk 1986, Cruden et al. 1999a/. Cross section B-B' was constructed by integration of 2.5 D forward models of residual gravity anomalies and field data. G = Gåsborn; L = Långban.*

2.1.3 Pluton floors

The characteristics of the floors of the two plutons described above are compared to those determined by other gravity studies in Figure 2-3 /Vigneresse 1995, Dehls et al. 1998/. Two first-order pluton floor geometries are observed /cf. Vigneresse et al. 1999/. As can be seen in Figure 2-3, wedge-shaped plutons have one or more root zones and can be symmetric (e.g. Pontivy, Cabeza de Araya) or asymmetric (e.g. Ljugaren, Mortagne). Their floors dip inward from very shallow angles, defining broad open funnel shapes (e.g. Nordmarka-Hurldalen) to steep angles, defining carrot-like shapes (e.g. Ulu). Tablet-shaped plutons are characterised by almost parallel roofs and floors and steep sides (e.g. Dinkey Creek, Graah Fjelde). Some plutons have both wedge and tablet-shape characteristics (e.g. Fichtelgebirge, Gåsborn). Almost all gravity studies find one or more funnel-shaped root zones that are interpreted to be feeder structures /e.g. Ameglio and Vigneresse 1999/.

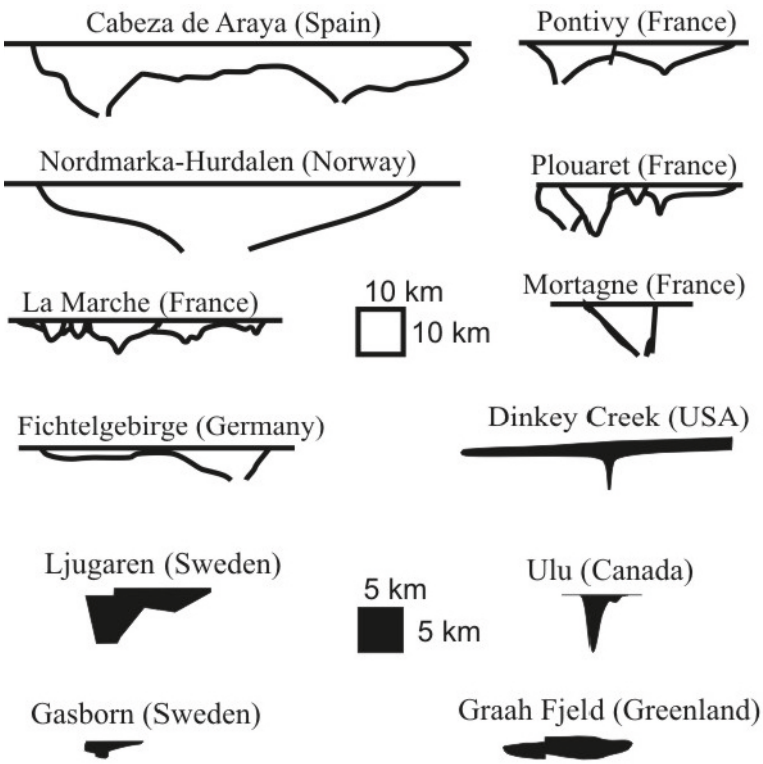

Figure 2-3. *Profiles of granitic intrusions determined from gravity and field observations. Data from /Vigneresse 1995 (unfilled profiles), Cruden and Aaro 1992, Dehls et al. 1998, Cruden et al. 1999ab, Grocott et al. 1999/. Note change of scale between unfilled and filled profiles.*

Field examples of the nature and geometry of plutons floors are relatively uncommon, for reasons discussed above. However, limited observations in Greenland, North and South America and the Himalaya /e.g. Hamilton and Myers 1974, Le Fort 1981, Scaillet et al. 1995, Skarmeta and Castelli 1997, Grocott et al. 1999/) are in general agreement with gravity models and seismic images of plutons floors. For example, several Proterozoic granites in South Greenland (e.g. Graah Fjeld and others /Grocott et al. 1999/) display well-exposed gently inward dipping bases that are often transgressive to wall-rock stratigraphy and in some cases show evidence for steepening towards a possible feeder zone /viz. Bridgewater et al. 1974/. Syn-emplacement ductile fabrics are developed in the footwall rocks of some of these intrusions (e.g. Quernertoq) that overprint pre-emplacement regional fabrics. Ductile shear bands in the footwall rocks of the Quernertoq intrusion, together with the geometry of the contact, were previously interpreted to indicate emplacement into an active extensional ramp-flat structure /Hutton et al. 1990/. However, Grocott and others /see discussion in Hutton and Brown 2000/ consider these to be local structural features related to depression of the pluton's floor. Similarly, /Hamilton and Myers 1974/ interpret map patterns associated with the base of the Boulder batholith, USA, to indicate that the intrusion is "bathtub-shaped" and that cuspate margin features represent lobes of granite that "flowed northward over the sinking floor". /Rosenberg et al. 1995/ have mapped in 3-D the floor of the Bergell pluton in the central Alps. Although the floor has a gentle regional dip, it has a more complex geometry due to syn-emplacement folding. In the Himalaya, the smaller Bhagirathi /Searle et al. 1993/ and Gangotri /Scaillet et al. 1995/ granites crop out as sub-horizontal lenticular bodies that may be controlled by flat-lying extensional structures. The larger Manaslu granite appears to post-date regional extension and has a lower contact that is "rather flat and parallel to the main metamorphic cleavage, with a transition zone, a few hundred metres thick, where the gneisses and marbles are cross-cut by a network of sills and dykes" /Guillot et al. 1993/.

2.1.4 Pluton roofs

/Paterson et al. 1996/ have reviewed the characteristics of pluton roofs exposed in the Cordillera of North and South America. These roofs consistently show gentle dips to slightly domal morphologies and discordant contact relationships with pre-existing wall-rock structures. Furthermore, emplacement-related ductile strain in the wall rocks is typically absent to poorly developed, and there is little evidence that the roofs have been lifted above their pre-emplacement position. Minor stoped blocks occur beneath the roof, and stoping is a likely candidate for generating the jagged profiles of the roofs, although its role as a major space-making mechanism is debatable, as discussed in Section 2. Other authors report more compelling evidence for upward displacements of pluton roofs /e.g. Benn et al. 1999, Grocott et al. 1999, Morgan et al. 2000, Saint Blanquat et al. 2001, Stevenson et al. 2007a/. Hence, roof uplift may be an important contributor to the space making process for some plutons, particularly in compressive and transpressive tectonic regimes, in which regional shortening can both aid in the roof-lifting process /e.g. Benn et al. 1998/ and act to squeeze magma upwards /e.g. Rosenberg et al. 1995/.

2.1.5 Pluton sides

Relatively undisturbed roofs, sharp transitions to steeply dipping walls, and the presence of either sharp wall-rock contacts or narrow strain aureoles with evidence for pluton-side-down shear have been used by /Paterson et al. 1996, Paterson and Miller 1998, Miller and Paterson 2000/ to argue that most space for emplacement of granites is due to downward transfer of material. Although these authors favour mechanisms such as stoping or return-flow during diapiric ascent, downward displacement and rotation of wall rock structural markers and fabrics towards the margins of intrusions in Greenland, Sweden and North America suggests that floor-subsidence may be an important space-making process /Bridgewater et al. 1974, Cruden 1998, Benn et al. 1999, Grocott et al. 1999, Brown and Mclelland 2000, Potter and Paterson 2000, Culshaw and Battnagar 2001/. Pluton-side-down shear sense indicators and roll-over of strata adjacent to some plutons have recently been ascribed to late-stage sinking of cooling magma bodies /Glazner and Miller 1997, Sylvester 1998, Morgan et al. 2000/. However, the observations

around these intrusions could also be attributed to syn-emplacement floor subsidence, possibly accompanied by a component of lateral expansion of the pluton margins /Cruden 1998/. Large scale tilting of roof pendants and wall rocks in the Sierra Nevada and Boulder batholiths has also been attributed to downdrop of pluton floors during batholith growth and emplacement /Hamilton and Myers 1974, Hamilton 1988, Tobisch et al. 2001/.

2.1.6 Internal structure of plutons

Where not overprinted by tectonic strains /e.g. Fowler and Paterson 1997/, mineral and magnetic fabric studies of granites often reveal concentric magmatic foliation and lineation patterns that define one or more possible feeder zones /e.g. Bouchez 1997, Cruden et al. 1999b/. These frequently correspond to the root zones defined by gravity data where it is available /e.g. Benn et al. 1999, Ameglio and Vigneresse 1999/. In some plutons, compositional zonation defines an annular pattern that is geometrically consistent with the presence of a feeder zone and indicates emplacement either as a series of nested pulses, or a progressive composition change in a more continuous magma input with time /e.g. Vigneresse and Bouchez 1997, Cruden et al. 1999b, Hecht and Vigneresse 1999/. Concentric structural patterns in plutons have also been delineated by finite strain analyses of deformed mafic enclaves and phenocryst distributions, e.g. Ardara granite (Holder 1979, Molyneux and Hutton 2000/ and Chinamora batholith /Ramsay 1989/. Finite strains are typically of general flattening type and increase in magnitude from the core to the margin of the pluton. Such data have been used to support pluton emplacement by a ballooning mechanism, although the amount of space created by this process is controversial, i.e. between 30 and 80% /see discussion in Molyneux and Hutton 2000/. As noted by /Cruden 1998/, the strain patterns in plutons ascribed to ballooning could also be produced by radial outward flow of magma from a central conduit into a horizontal widening and vertically thickening tabular body /see also Hunt et al. 1953/.

There is increasing evidence that some plutons, including those that are macroscopically homogeneous, are made up of many m- to km-scale sheets /e.g. McCaffrey 1992, Everitt et al. 1998, Cobbing 1999, Glazner et al. 2004/. Detailed textural observations of intrusions in Maine, SW Australia and S New Zealand suggest that initially sub-horizontal sheets steepen with time during growth of a pluton /Wiebe and Collins 1998/. This is supported by U-Pb studies in the Coast Plutonic Complex, where plutons are interpreted to have grown from the floor upward by stacking of sheets and gradual subsidence and distortion of their floors /Brown and Walker 1993, Brown and McClelland 2000/.

2.1.7 Empirical power law

/McCaffrey and Petford 1997/ proposed that both plutons and laccoliths display a scale invariant relationship between their thickness (T) and width (L) that can be described by a simple power law of the form:

$$T = bL^a \quad (1)$$

Major axis regression on log T vs. log L plots determined an intercept (b) value of 0.12 and slope (a) of 0.88 for 135 laccoliths. Although the fit for laccoliths seemed quite robust, /McCaffrey and Petford's 1997/ result for plutons was based on only 21 observations. In order to better characterise the power law scaling of plutons, /Cruden and McCaffrey 2001/ utilised 66 studies of individual plutons, the majority (48) of these studies involved gravity surveying methods, and the remainder (18) employed field-based methods. They define the horizontal dimension of a pluton (L) as the equivalent diameter of a circle given by measurements of either the major and minor axes of elliptical bodies or their areas, and the thickness (T) is as the mean value where data are sufficient. The resulting data set (Figure 2-4) spans over two orders of magnitude, from small plutons such as the Gåsborn granite (L = 4.5 km, T = 1.6 km /Cruden et al. 1999a/) to large single plutons like the Lucerne granite (L = 56 km, T = 4.5 km, /Sweeney 1976/) and composite batholiths such as the Sierra Nevada (L = 600 km, T = 15 km /Oliver 1977/). There is no obvious difference between pluton dimensions determined by field and geophysical methods,

except for very large intrusions with $L > 50$ km, which are too large to provide field-based means for thickness estimation. Major axis regression of the pluton data yields a power law relationship (Equation 1) with a reasonable fit to the data characterised by an intercept value, $b = 0.6$ (± 0.15) and a slope, $a = 0.6$ (± 0.1). Error limits describe variation in the data at the 95th percentile level and define a field in log T vs. log L space that incorporates most of the observations (Figure 2-4).

The power law scaling of laccoliths has also been re-evaluated in light of more recent studies of laccolith geometries in distinct geological settings, e.g. Elba /Rocchi et al. 2004/. When laccoliths groups are examined on a geographic basis, a power law slope a ~1.5 appears to better describe the geometry of this class of intrusion /Cruden and McCaffrey 2002/. The revised power law scaling curve for laccoliths based on this analysis, with 95% error limits, is also plotted in Figure 2-4.

Comparison of the pluton and laccolith data and their respective power laws indicates that both populations represent distinct geometric classes of intrusion, which likely reflects different emplacement mechanisms (e.g. floor depression vs. roof lifting; see below) and emplacement depths (mid-crust vs. shallow crust). Areas of overlap between each group on Figure 2-4 probably represent transitional types of intrusion. Some plutons, such as the anomalously thin Mount Scott granite /Hogan and Gilbert 1995/, the Glenmore granite /Talbot and Grantham 1987/ and the stratoid granites of Madagascar /Nédélec et al. 1994/ are more appropriately regarded as laccoliths or sills, based on their L/T ratios.

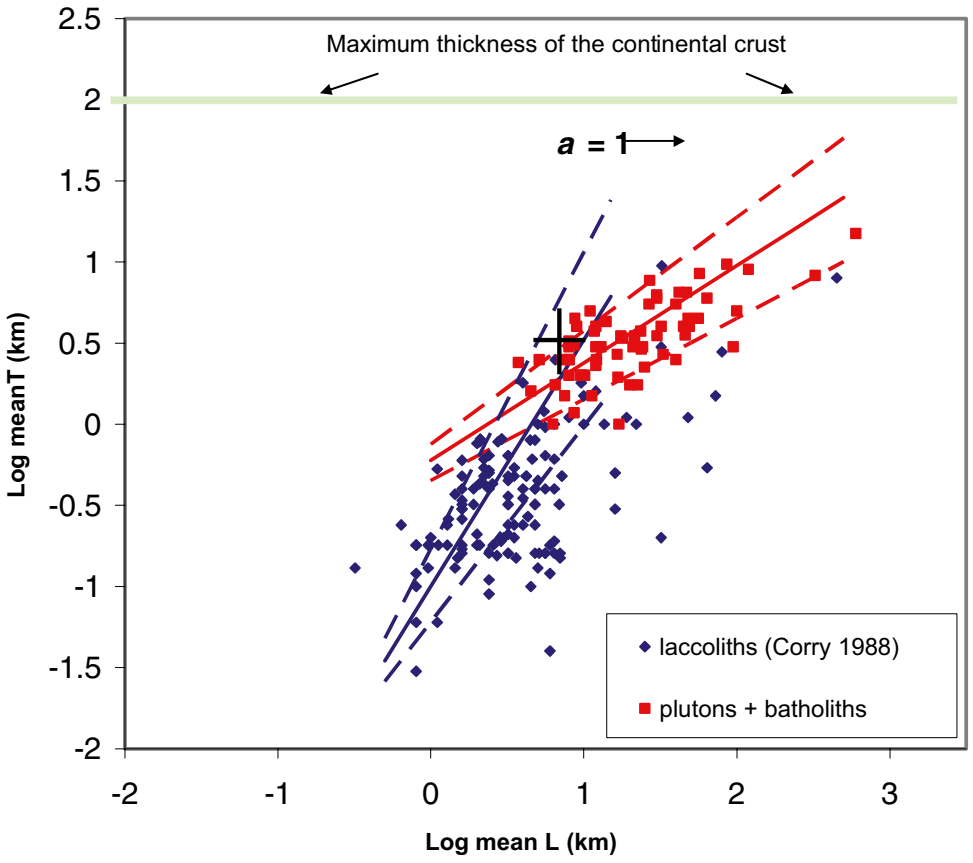

Figure 2-4. *Log thickness (T) vs. log length (L) data for 66 plutons and 135 laccoliths as determined using geophysical methods and by field observations. Best-fit slopes (thick solid red and blue lines) and their 95th percentile confidence limits (dashed lines) were determined by reduced major axis regression /McCaffrey and Petford 1997, Cruden and McCaffrey 2001, 2002/. The slope for a self-similar relationship between T and L (a = 1) and the maximum thickness of continental crust (100 km) are shown for comparison. Black cross indicates dimensions of the Götemar and Uthammar granites based on this study.*

2.2 Granite ascent and emplacement mechanisms

The granite plutons reviewed above share three fundamental characteristics: their shape, power law size distribution and tabular to wedge geometry. The degree of ductile wall-rock deformation associated with intrusion appears to be a function of emplacement depth and the mechanical properties of the host during emplacement. Plutons emplaced in a ductile environment show evidence for components of lateral and vertical displacement of wall rocks, whereas those emplaced in brittle environments can only have involved vertical translation of wall rock material, due to absence of wall-rock strains. Deeper level, isolated granites with well-defined Bouguer gravity anomalies often have model shapes with flat to gently inward dipping floors and one or more roots, but no exposed roof. Higher level intrusions preserve discordant flat roofs, steep sides and rare, but significant evidence for gently inclined floors. Reasonable generalisations for many, but not all, granites are therefore that they are emplaced as tabular to wedge-shaped bodies with thicknesses ranging from 1 to 10 km, they are fed by one or more vertical conduits, the bulk of magma flow at the emplacement level is horizontal, and that the role of lateral displacement in creating space diminishes with decreasing ductility of the wall rocks. Any ascent and emplacement mechanism must account for these characteristics.

2.2.1 Diapirism

Tabular to wedge shaped bodies of granite can form by impingement and spreading of a diapir, which has been arrested by a gently inclined mechanical barrier /e.g. Brun and Pons 1981, Cruden 1990/ or by injection and subsequent thickening of a sill fed by a dyke /Pollard and Johnson 1973, Brisbin 1986, Corry 1988, McCaffrey and Petford 1997/. Evidence for lateral ductile displacement of wall rocks has been discussed above and is permissible evidence for spreading diapirs. However, it was also noted that the narrowness of the deformation aureole and the strain magnitude within it are unexpectedly low for a diapiric mechanism /Paterson et al. 1991, Paterson and Fowler 1993/. Narrow strain aureoles around some plutons may still be accounted for by diapiric ascent if thermal softening /Marsh 1982, Mahon et al. 1988/ and/or strain rate softening /Weinberg and Podlachikov 1994/ behaviour occurs in the wall rocks. Although these models result in narrower strain aureoles than those predicted for diapiric ascent under isothermal, linear rheological conditions /Schmeling et al. 1988/, they will generate even higher strain intensities within the aureole, which have not been observed. More recently, ascent of "viscoelastic diapirs" has been proposed /Paterson and Miller 1998/, based on /Rubin's 1993/ analysis of dyke propagation through a medium with variable viscous and elastic properties. /Paterson and Miller 1998/ envisage a spectrum from diapiric blobs with narrow ductile strain aureoles, through diapiric ridges with even narrower aureoles to discordant dykes. The problem of insufficient strain record still remains for diapirs and diapiric ridges, as does that of slow ascent rates that preclude long distances of magma ascent before freezing /Mahon et al. 1988/. Dyke transport is discussed further in Section 2.2.3 below.

2.2.2 Stoping

A complete absence of wall-rock strain around higher level discordant plutons precludes spreading of diapirs as a viable mechanism for their emplacement. Stoping is often invoked to explain the ascent and emplacement of such discordant intrusions /e.g. Barrell 1907, Paterson et al. 1996, Clarke et al. 1998/. However, energetic and thermal considerations suggest that stoping is unlikely to allow transport of granite magma more than a few thousand meters before freezing /Marsh 1982, 1984/. Furthermore, it is difficult to envision how magma ascending from its source by stoping would result in a tabular geometry at the level of final crystallisation. Stoping is therefore considered to be an important process in the modification of the roofs and walls of high-level intrusions, and although it may account for the last few 100's of metres of magma ascent, it is probably unimportant for crustal-scale magma transport.

2.2.3 Channelled magma ascent

A long-standing objection to the dyke transport of granite was that high viscosity magma would freeze in the dyke before a volume sufficient for filling a pluton could travel through it /Marsh 1982/. However, it is now realised that felsic melts have viscosities in the range 10^3–10^7 Pas /Clemens and Petford 1999, Dingwell 1999/. Consequently, dyke transport of felsic magma may be sufficiently rapid to prevent freezing, and furthermore, pluton-sized upper crustal chambers can be filled by dykes over geologically rapid times /Petford et al. 1993, Petford 1996, Cruden 1998/. Alternative, but still rapid, mechanisms for channelled flow of low viscosity magma are transport within mobile hydrofractures /Weertman 1971, Bons et al. 2001/ and pervasive flow /Brown 1994, Collins and Sawyer 1996, Weinberg and Searle 1998, Leitch and Weinberg 2002/. In the former, a penny shaped, magma filled crack ascends buoyantly by simultaneously propagating its tip and closing its tail. Dykes differ from hydrofractures in that they must stay open from top to bottom. Recent experimental work on hydrofractures suggests that they may allow step-wise accumulation of magma pulses into a pluton, leaving very little trace of their ascent in the underlying crust /Bons et al. 2001/. During pervasive flow, magma ascends upwards through an extensive network of channels which are formed by active deformation and kept open by a combination of dilatant strain and magma pressure /Collins and Sawyer 1996, Brown and Solar 1998/. This results in an intrusive migmatite terrain or injection complex, that may be capped by tabular granites /e.g. Weinberg and Searle 1998/. Recent one-dimensional thermal modelling /Leitch and Weinberg 2002/ has shown that magma can flow pervasively as long as the host rock is above the magma solidus. Although incoming magma has the potential to push isotherms further up in the crust, transport by pervasive flow seems to be limited to only several kilometers in the lower to middle crust. Because dyke transport lies in between hydrofracturing and pervasive flow, in the sense that hydrofractures involve rapid, crust-traversing transport and pervasive flow involves dispersed, short range transport and connectivity between source and pluton, and because dyking is relatively better understood process, we will assume this mechanism for granite magma transport below and in the following sections.

2.2.4 Laccoliths vs. lopoliths

The driving force for dyke transport is normally assumed to be buoyancy, however, both internal magmatic and tectonic over-pressuring /Robin and Cruden 1994, Hogan et al. 1998, Brown and Solar 1998/ are also attractive mechanisms for forcing magma up through vertical conduits. Vertically propagating magma dykes must be arrested and thereafter be able to propagate horizontally in order to form a sill. Arresting mechanisms or "crustal magma traps" have been reviewed by /Brisbin 1986, Corry 1988, Clemens and Mawer 1992, and Hogan et al. 1998/ and include intersection with a freely slipping horizontal fracture, stopping of the propagating dyke by a ductile horizon or a unit with high fracture toughness, and arrival at a level of neutral buoyancy. Once an initial sill has formed, it can inflate provided a sufficient magma pressure is available /Johnson and Pollard 1973, Pollard and Johnson 1973, Corry 1988/. Vertical inflation to plutonic dimensions can occur by roof lifting (i.e. laccolith emplacement), floor depression (i.e. lopolith emplacement) or a hybrid mechanism (Figure 2-5) /Cruden 1998, 2006/. The dynamics of laccolith emplacement by roof lifting are well-established /Pollard and Johnson 1973, Jackson and Pollard 1988, Corry 1988/. Most models assume a two-stage process involving the formation of an initial sill following by vertical growth. Both stages are driven by the overpressure of magma at the emplacement site.

Field and theoretical considerations show that vertical growth of laccoliths occurs by elastic, elastic-plastic or ductile bending of the roof rocks /e.g. Johnson and Pollard 1973, Pollard and Johnson 1973, Dixon and Simpson 1987, Roman-Berdiel et al. 1995/, lifting of a piston by displacement on faults /e.g. Corry 1988/, or a combination of these mechanisms (Figure 2-5 /Jackson and Pollard 1988/). Note that "space creation" here is ultimately accommodated by surface uplift and subsequent erosion. The amount of vertical growth is a function of the horizontal cross sectional area of the laccolith, the strength and effective thickness of the roof rocks, and the available driving pressure /Pollard and Johnson 1973, Dixon and Simpson 1987/.

It would appear that laccolith growth is self-limiting and rarely exceeds 2 km /Corry 1988/. The power law scaling of laccoliths is an expression of the limits placed on vertical growth, in which the force available for roof lifting is a function of the magma driving pressure and the area of the initial sill /McCaffrey and Petford 1997, Cruden and McCaffrey 2002/. Further growth requires either rapid removal of the roof at the surface by erosion or gravity collapse, or simultaneous depression of its floor.

With the exception of mid-crustal plutons in which roof lifting was aided by tectonic compression, most studies consider laccoliths to be shallow level intrusive phenomena, with all documented examples occurring at paleodepths < 3 km /Corry 1988/. Experimental work suggests that the aspect ratios of laccoliths increase with depth. This is because horizontal sill propagation or growth is favoured over roof lifting with increasing overburden thickness /Roman-Berdiel et al. 1995/. /Corry 1988/ proposes that at greater depths lopoliths form and that there is a continuous transition between intrusive styles from the epizone to the mesozone (Figure 2-5). Although the depth of this transition is not well constrained, it is noteworthy that the majority of the granitic plutons discussed in above were emplaced at paleodepths > 3 km. The structural and geophysical attributes of these intrusions, suggest that many plutons are geometrically similar to lopoliths (Figure 2-3). However, the form and wall-rock structure of lopoliths are inferred to have formed by downward sagging of wall rocks after intrusion of the magma /Corry 1988/. The model proposed below is that space for incoming granitic magma is made by depression of the floor during intrusion.

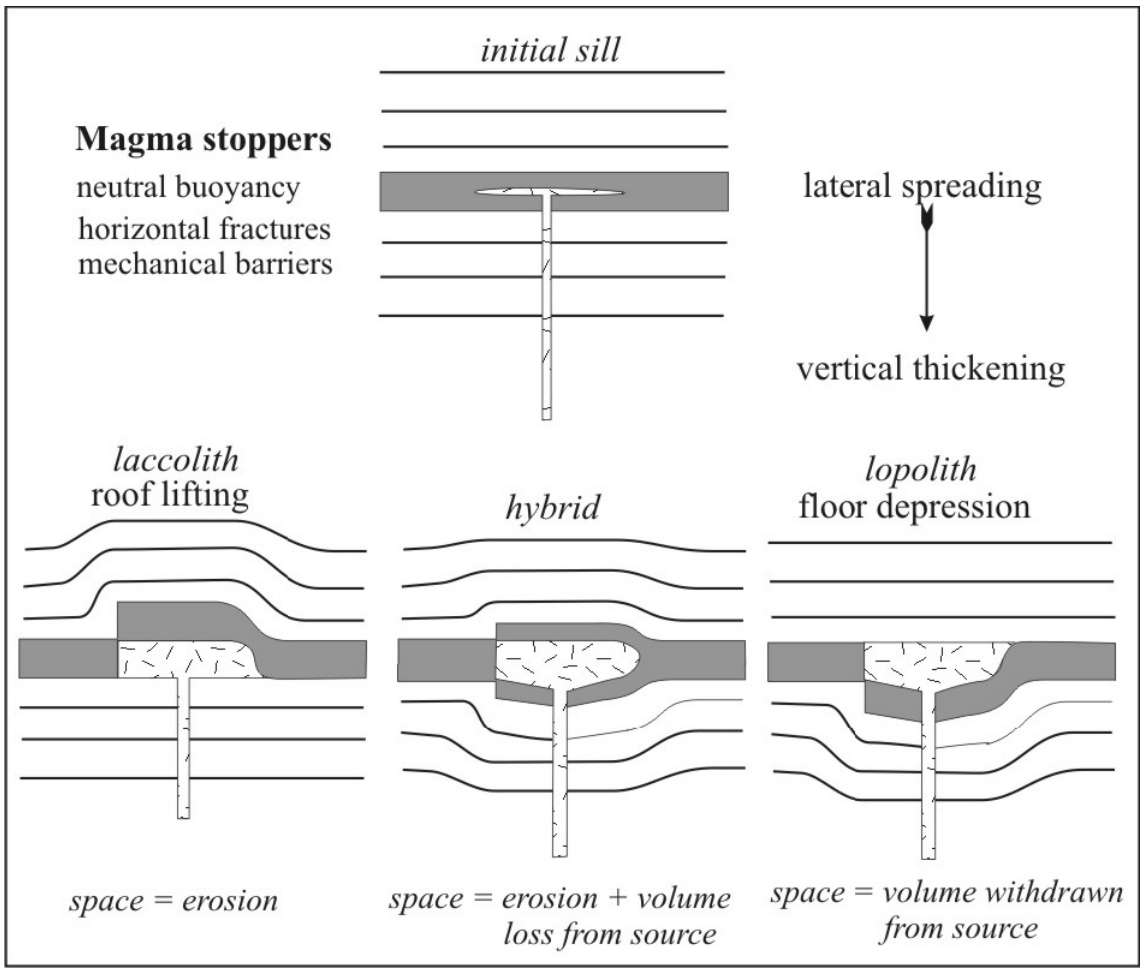

Figure 2-5. *Modes of tabular granite emplacement. On the left hand side of each diagram space for the granite (shaded) is created within the intruded unit (stippled) by offsets on faults, whereas space is created by ductile deformation on the right hand side of each diagram. From /Cruden 1998, Cruden 2006/.*

2.2.5 Pluton emplacement by floor depression

Floor depression, or subsidence, has been considered as a possible space-making mechanism for granites for almost 100 years /Clough et al. 1906, Cloos 1923, Hamilton and Myers 1967, Lipman 1984/. Most early models for whole-scale subsidence of pluton floors during emplacement invoked the presence of a magma chamber or reservoir in the lower crust /Branch 1965. Whitney and Stormer 1986/ or in the crust underlying the growing intrusion /Myers 1975, Bussell et al. 1976, Pitcher 1979/. In such "cauldron subsidence" models the intervening crust is assumed to drop down into an underlying magma chamber, usually guided by pre-existing fractures. Downward displacement of plutons floors by ductile flow mechanisms has also been discussed /Hamilton and Myers 1967, Brown and Walker 1993/, possibly aided by isostatic depression of the Moho /Brown and McClelland 2000/. More recent models for floor depression take into account the notions that granitic magmas are likely extracted from partially molten lower crust /e.g. Brown 1994, Thompson 1999/, that magma transport is likely to be channelled and rapid, and that the rates of melt extraction, ascent and emplacement must be balanced at the crustal scale /Cruden 1998, 2006/.

Figure 2-6 illustrates schematically how pluton growth in the upper to middle crust by floor depression may be accommodated by volume loss due to melt withdrawal in the lower crust. The crustal column between the growing emplacement site and the source can be viewed as foundering into a deflating layer of partial melt, and the volume of melt lost from the lower crustal reservoir must be balanced by the volume emplaced in the pluton. Hence, the volumetric withdrawal rate in the source, Q_W, and the volumetric flux in the feeder dyke (or dykes), Q_A, and the volumetric filling rate of the pluton, Q_E, must all be equal (Figure 2-6).

In Figure 2-6 melt is extracted from a source volume restricted to the volume directly beneath the pluton, which (arbitrarily) grows asymmetrically via a feeder on one side. Deflection of originally horizontal markers below the intrusion indicates that floor depression must be accommodated by deformation of the crust between the source and the growing pluton, and within the source itself. In this model the pluton is inferred to deepen towards the feeder, in accord with the floor geometry determined in many geophysical studies (Section 2.1.3, Figure 2-3). Such geometry might arise due to differential melt withdrawal and resulting subsidence in the source. If melt extraction is driven primarily by density driven flow into a conduit, then differential melt withdrawal will be a natural consequence of decreasing melt flow velocities away from the evacuation point. When melt is withdrawn from a source directly below the pluton (Figure 2-6), the degree of partial melting must be very high, or the thickness of the source must be substantially greater than the final thickness of the intrusion. For the geometry sketched in Figure 2-6, about 25% of the source's original volume must be extracted in order to grow the overlying pluton.

The dynamics of this process in anorogenic settings have been evaluated by /Ablay et al. 2008/ who propose a model that accounts for both the generation of fractures that allow for removal of melt from the source and a buoyancy pumping mechanism that aids in the transport of melt to the emplacement site. Structural accommodation mechanisms and their interaction with regional tectonic processes and structures are reviewed further by /Cruden 2006/.

The transport of melt from a lower crustal source and growth rates of plutons are potentially geologically rapid processes with theoretically predicted pluton filling times of years to hundreds of thousands of years /Cruden 1998, Petford et al. 2000, Ablay et al. 2008/. However, if magma is delivered to the emplacement site in discrete pulses, cumulative pluton growth times can occur over several millions of years if the time gap between pulses is large /Cruden and McCaffrey 2001/. This theoretical prediction is supported by recent field, geochronological and thermal modelling studies of plutons /Glazner et al. 2004, Coleman et al. 2004, Annen et al. 2006/.

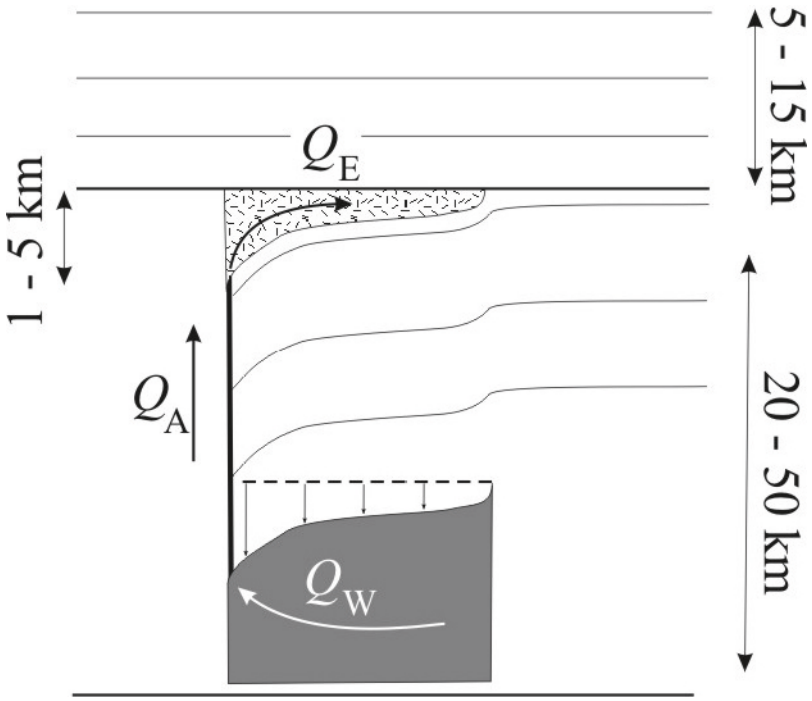

Figure 2-6. *Hypothetical scenario for pluton emplacement by floor depression driven by withdrawal of melt from an underlying source region. The pluton (stippled) is asymmetric and fed by a conduit located on one side. Melt is withdrawn differentially from a partially molten source (shaded) whose area is confined to the area below the pluton. Solid lines are initially horizontal markers. Dashed line above source indicates its original thickness. Thickness ranges of roof rocks, the pluton and the underlying crust are approximate and not shown to scale. Arrows indicate the flow of melt within the system, and the definitions of extraction (QW), ascent (QA) and emplacement (QE) flow rates. From /Cruden 2006/.*

3 Götemar and Uthammar Granites

3.1 Methodology and data Sources

The study has included:

1) review of relevant literature on the geology and tectonics of southeast Sweden and the Laxemar-Simpevarp area (SKB reports, journal articles);
2) field observations of the Götemar and Uthammar intrusions made on June 27 and 28, 2007, and previous observations made in July and August 1985 in the area north of Klintemåla (Misterhults skärgård /Cruden 1986, unpublished data/);
3) interpretation of regional aeromagnetic data; and
4) 2.75 dimensional forward modelling of terrain corrected Bouguer gravity data, constrained by petrophysical and borehole data (SKB reports).

Geological structures were measured with a compass clinometer and magnetic susceptibility readings were recorded with a hand held susceptibility meter. Structural data was compiled, plotted and analysed using Spheristat 2.2 (Pangea Scientific). Gravity data was processed using Oasis Montaj (Geosoft Inc.) and 2.75D forward modelling of residual gravity anomalies was carried out with GM-SYS. Annotation of regional aeromagnetic data was done using CorelDraw 13.0.

3.2 Regional Setting

The c. 1.45 Ga Götemar and Uthammar intrusions /Kresten and Chyssler 1976, Åhäll 2001/ were emplaced into plutonic rocks of the c. 1.80 Ga generation of the Transcandinavian Igneous Belt (TIB) (Figure 3-1). The study area is located south of the NW-SE trending boundary between the TIB and the commonly metamorphosed intrusive and supracrustal rocks to the north in the Paleoproterozoic Svecokarelian orogen. The main period of ductile deformation in the bedrock in the Svecokarelian orogen occured between c. 1.85 and 1.75 Ga followed by post-orogenic events under increasing lower metamorphic grade conditions until c. 1.5 Ga /Beunk and Page 2001/. The c. 1.86–1.75 TIB rocks are affected by the Svecokarelian orogeny. Aeromagnetic data indicates the presence of an anastomosing system of regional shear zones in the TIB with similar orientation to those in the the Svecokarelian orogen to the north (Figure 3-2). The principal orientation of aeromagnetically defined shear zones is WNW-ESE, which are interpreted to have dextral shear sense based on offsets of magnetic markers. An important secondary shear zone orientation trends NE-SW, particularly in the Oskarshamn-Äspö area. This secondary set is interpreted to be conjugate to the WNW-ESE trend, in agreement with observations of sinistral shear sense in NE-SW shear zones in the Laxemar-Simpevarp area /Lundberg and Sjöström 2006/.

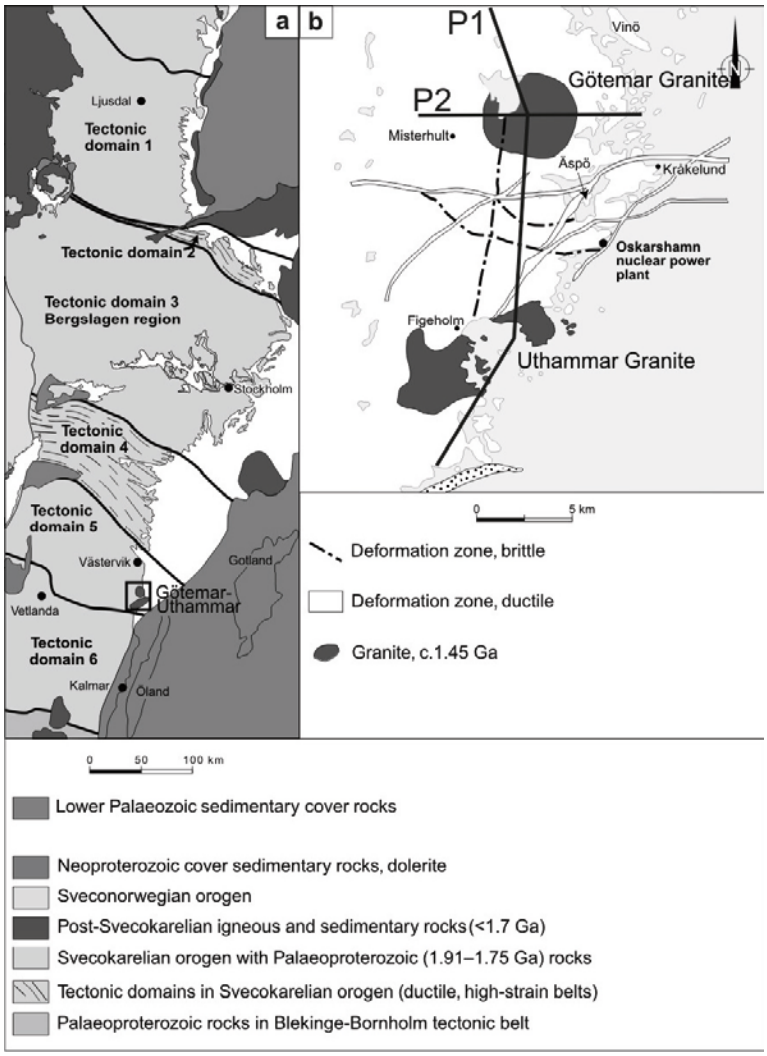

Figure 3-1. *(a) Regional geology map of SE Sweden showing major tectonic domains of the Svecofennian Orogen and the locations of the study area (box). (b) Simplified geological map of the Götemar and Uthammar plutons showing locations of gravity profiles P1 and P2.*

The Götemar and Uthammar granites are part of a suite of c. 1.45 Ga plutons that occur in the southwest Baltic Sea region. These intrusions are well defined aeromagnetically by circular to elliptical anomalies (Figure 3-2). Most of these anomalies indicate that the c. 1.45 Ga plutons are unexposed or covered by Paleozoic sedimentary sequences and relatively few (e.g. Götemar, Uthammar and Jungfru granites) are exposed. Preliminary interpretation of the aeromagnetic data suggests that the anorogenic plutons occur in a NNE-SSW trending linear belt that boarders the SE coast of Sweden. This observation suggests a deep-seated tectonic control on the location and emplacement of c. 1.45 Ga plutons, such as the Götemar and Uthammar granites. Similar linear distributions of high-level laccolithic intrusions are observed in the Mesozoic-Tertiary of western North America (e.g. Iron Axis, Henry Mountains /Corry 1988/).

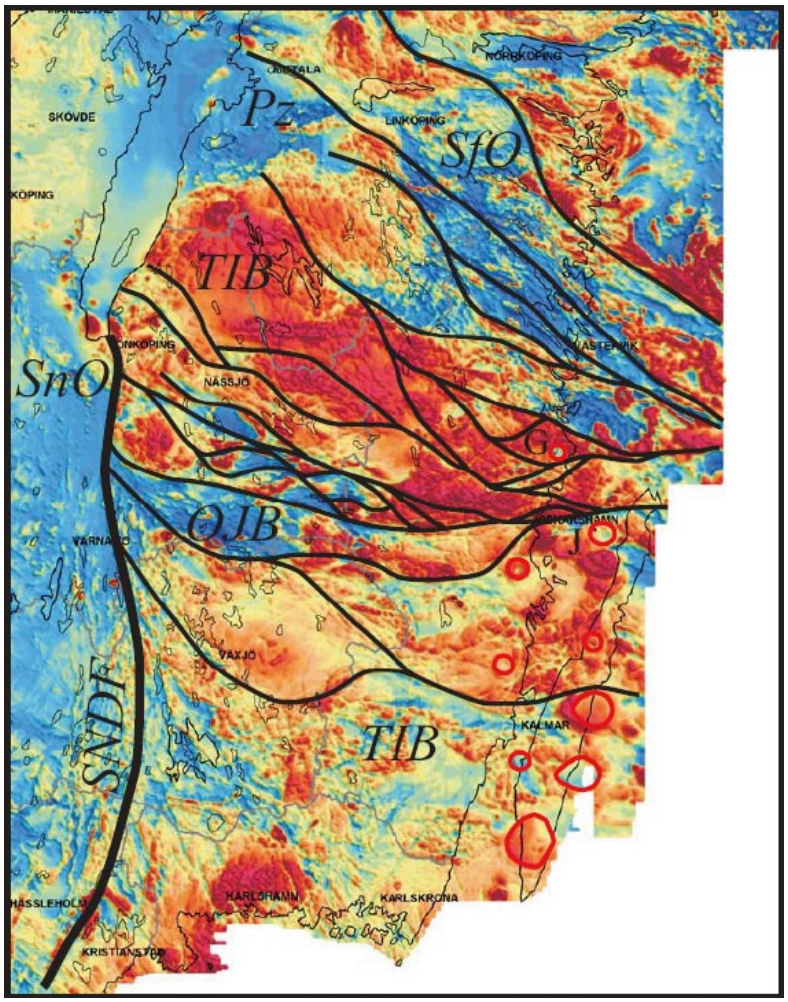

Figure 3-2. *Total field aeromagnetic anomaly map of SE Sweden (provided by the Geological Survey of Sweden). Thick black lines are interpreted shear zones. Close red lines are interpreted c. 1.45 Ga granite intrusions. SfO = Svecofennian Orogen; SnO = Sveconorwegian Orogen; TIB = Transcandinavian Igneous Belt; SNDF = Sveconorwegian Deformation Front; G = Götemar granite.*

3.3 Field Observations

Two days were spent in the field examining outcrops in and around the Götemar and Uthammar intrusions. Foliations were measured with a compass clinometer and magnetic susceptibility readings were recorded with a hand held susceptibility meter.

Both the Götemar and Uthammar intrusions are coarse-grained, brick red weathering, k-feldspar megacrystic granites. They have massive texture and only rarely display preferred orientation of k-feldspar megacrysts. Magnetic susceptibility is below the level of detection of the susceptibility meter employed in the field, indicative of very low values. The Götemar intrusion also contains aplites, which vary in width from a few centimetres to 10's of meters. The aplites occur as sheets of unknown dip. Differential weathering causes the aplites to crop out in arcuate ridges that trend sub-parallel to the pluton margins. One meter-wide aplite sheet observed west of the southern end of Götemar is oriented 140/40 SW, that is, dipping outward toward the pluton margin.

The Götemar and Uthammar granites intrude medium- to coarse-grained granites to quartz monzodiorites of the TIB. These rocks contain weak to moderate intensity metamorphic foliations defined by the preferred orientation of mafic minerals, feldspars, mafic inclusions and schlieren. Foliations are subvertical where observed and have peak strikes oriented NE, EW and ESE (Figure 3-3b). The EW and ESE foliation peaks observed in outcrops adjacent to both granites are similar to measurements collected to the north of the Götemar granite (Figure 3-3a, Misterhults Skärgård) and in the Laxemar-Äspö area /Wahlgren et al. 2006/. The orientation data peak in Figure 3-3b trending NE is largely due to measurements collected SE and E of the Götemar granite, and represents the regional structural trend in that area.

Wall rock outcrops were observed as close as 5 m to the margins of the Götemar and Uthammar granites. In every instance there is no evidence for ductile deflection or rotation of foliations, nor are there overprinting fabrics related to intrusion of the plutons. Hence it is concluded that both intrusions are discordant to their wall rocks. That is they cut cleanly across wall rock structures and impose no ductile deformation.

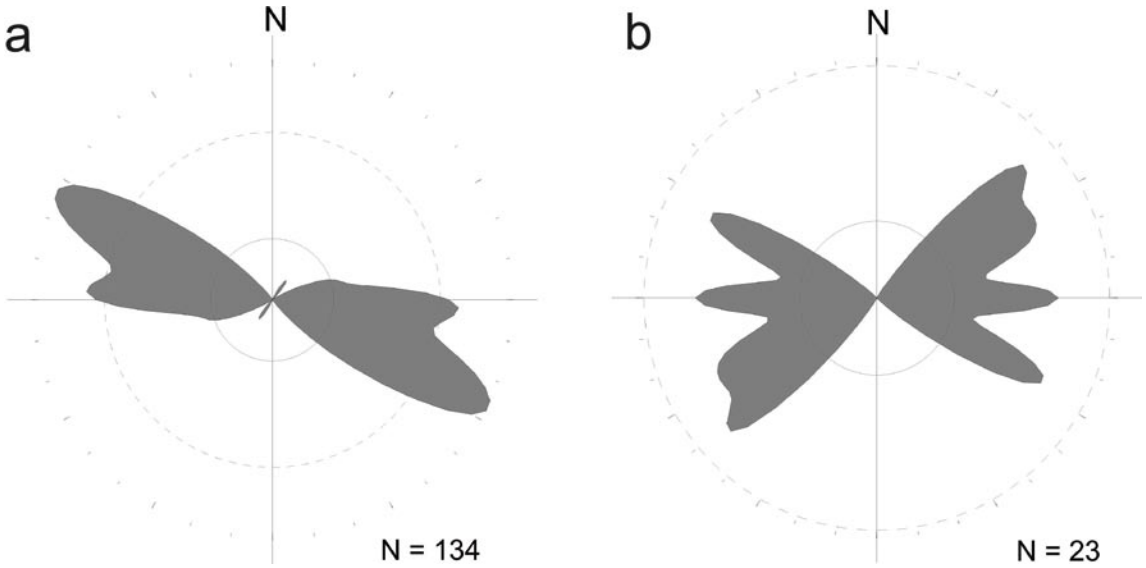

Figure 3-3. *Rose diagrams of foliation strike orientations. (a) Hamnö-Örö area, north of Götemar granite. (b) Wall-rocks surrounding Götemar and Uthammar granites. The inner solid circle is the expected frequency if all foliations measured were distributed evenly around the compass; all orientation peaks outside the inner solid circle are statistically significant. The outer dashed circle is the 95% confidence level for peak significance.*

3.4 Depth of Emplacement

$^{40}Ar/^{39}Ar$ cooling ages allow some constraints to be placed on the depth of emplacement of the Götemar and Uthammar granites. According to /Page et al. 2007, Söderlund et al. 2008/ the wall rocks cooled past the hornblende closure temperature of 500° C at c. 1.76 Ga and the biotite closure temperature of 300°C at c. 1.62 Ga. A linear cooling line through these ages yields the equation:

$$T = 1.1111t - 1500 \quad (2)$$

where T is temperature in °C and t is age before present in Myr. Extrapolation to the emplacement age of the Götemar and Uthammar granites at c. 1.45 Ga yields a lower bound estimate for the pre-emplacement wall rock temperature of 113°C. Taking a conservative continental geothermal gradient of 25°C/km gives an estimated emplacement depth of 4.5 km. If cooling was non linear, the wall rock temperatures may have been higher at 1.45 Ga. Taking a pre-emplacement wall rock temperature of 200°C yields an emplacement depth of 8 km. Despite the uncertainties, it can be concluded that the Götemar and Uthammar granites were emplaced at shallow crustal levels and significantly above the brittle-ductile transition.

3.5 Gravity Modelling

Terrain corrected Bouguer gravity data collected by /Nylund 1987/ and /Triumf 2004/ were compiled in Geosoft database format using the program Oasis Montaj. A Bouguer gravity anomaly map of the 1,295 stations was produced using the minimum curvature method (Figure 3-4). In order to visualise anomalies in coastal areas (e.g. Uthammar granite), contouring was carried out over a rectangular area defined by the limits of the gravity stations. However, due to lack of stations, anomalies in the south east area of the map are not well constrained.

The residual gravity anomalies of the Götemar and Uthammar granites were separated using the gravity station censoring technique of /Mickus et al. 1991/ which is particularly effective in insolating the gravity effects of geologically well defined objects, such as granites, in areas where the regional field is poorly defined or not known /Nitescu et al. 2003/. The method involves removing all gravity stations from the database that overlie the features of interest. The key criterion for the censoring method is for stations in the area affected by local anomalies to be removed. In this study the areas are defined by the iso-contours that form the external boundaries of the regions of high horizontal gradient that mark the bases of the Bouguer anomalies associated with the Götemar and Uthammar granites. Once removed, the censored Bouguer gravity data is re-gridded to produce a censored Bouguer gravity anomaly map (Figure 3-5). Subtraction of the censored and original Bouguer anomaly maps results in a residual gravity anomaly map of the two granites (Figure 3-6).

Both granites are associated with strong residual gravity anomalies (max. –100 G.U. or -10 mGal). The residual anomaly for the Götemar granite is better defined than that of the Uthammar pluton due to better gravity station coverage, and defines a bulls-eye contour pattern centred on the intrusion with a 0 G.U. (0 mGal) contour located ~3 km outside the pluton margin. As noted above, due to the absence of gravity stations offshore, the residual anomaly pattern of the Uthammar granite extending south east from the coast is not well constrained and its geometry in this area is likely an artefact of the contouring routine and the limits of the data set.

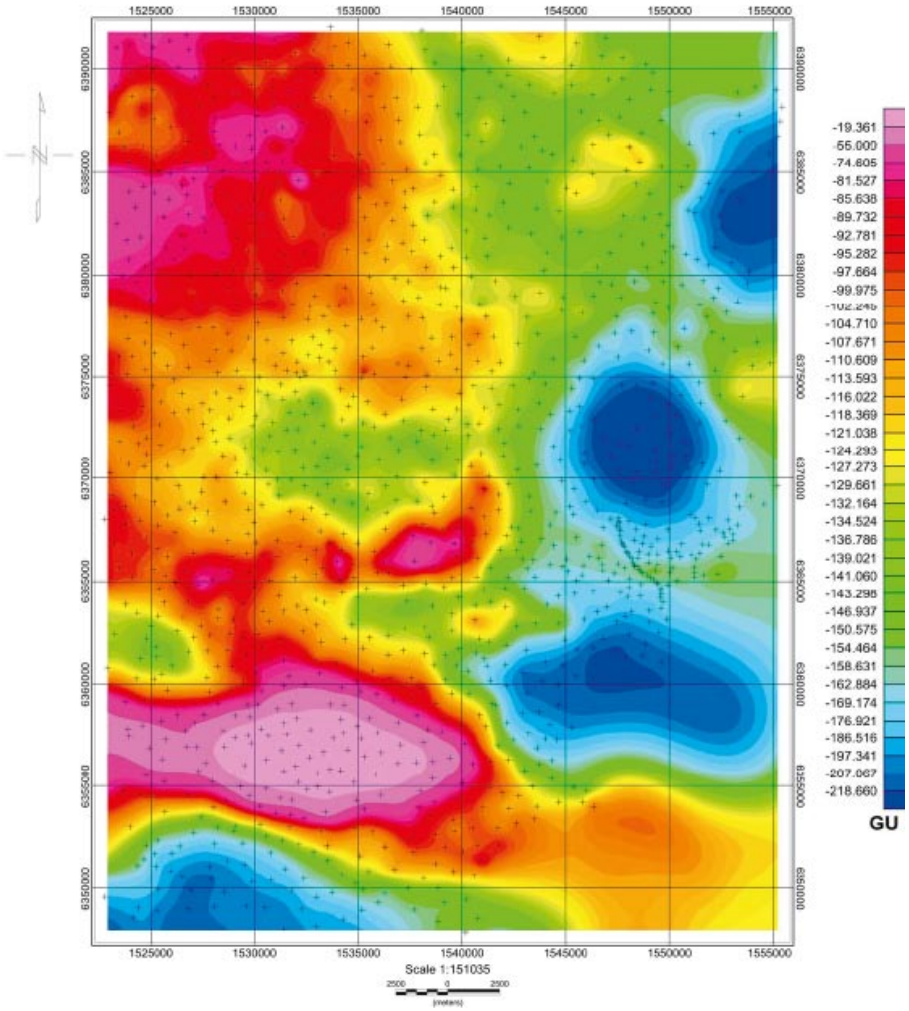

Figure 3-4. *Terrain corrected Bouguer gravity anomaly map of the study area. Contoured using the minimum curvature method. Crosses are gravity stations, Gravity Units (GU).*

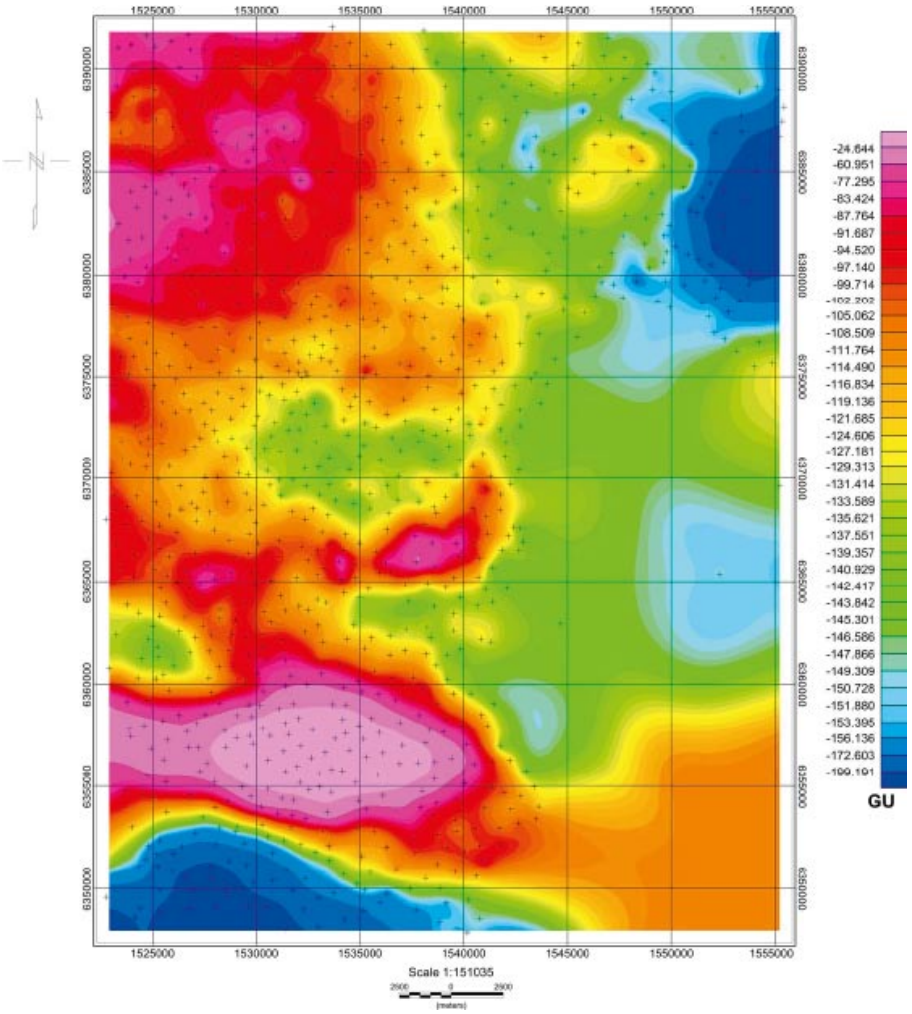

Figure 3-5. *Censored Bouguer gravity anomaly map for the study area. Contoured using the minimum curvature method. Crosses are gravity stations.*

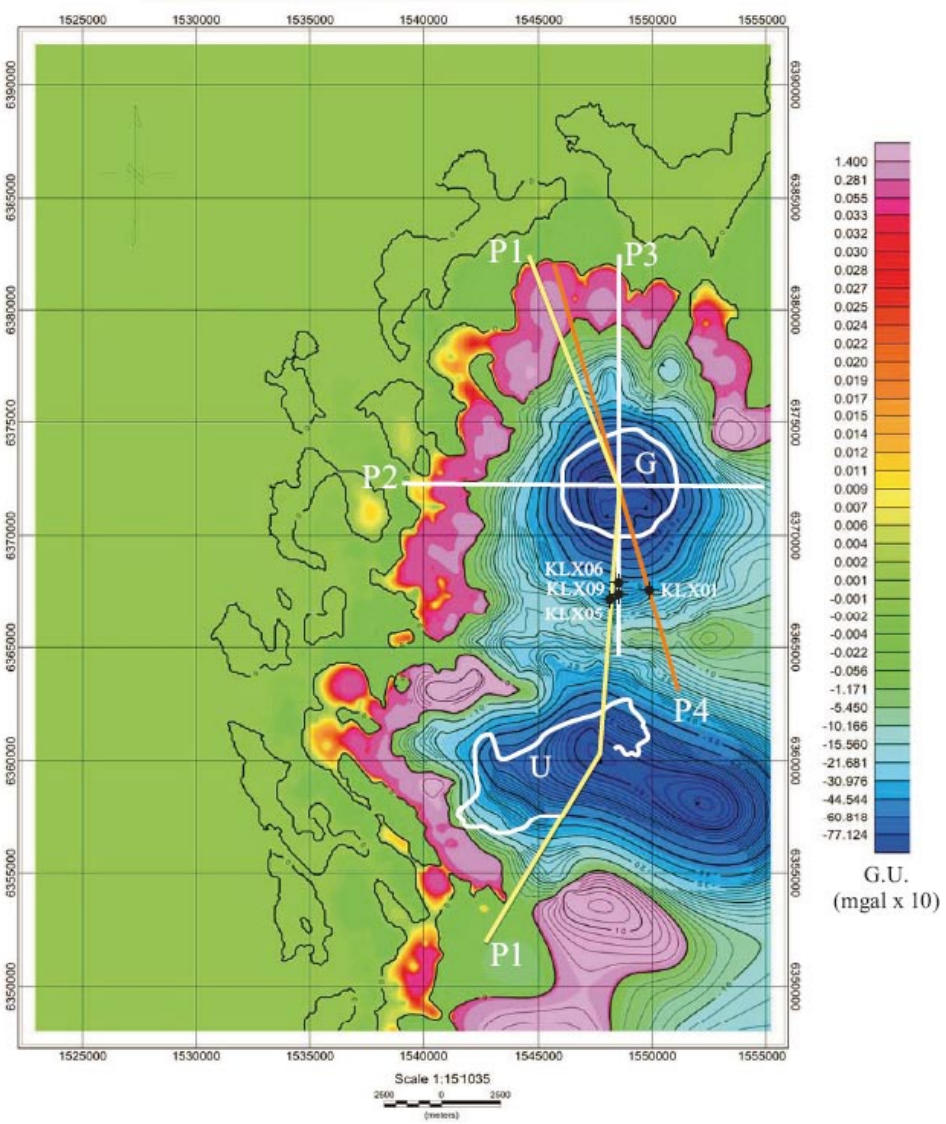

Figure 3-6. *Residual gravity anomaly map of the study area. Outlines of Götemar and Uthammar granites are shown as are the locations of gravity model profiles and boreholes used in their evaluation.*

The profiles of the residual field show clearly a break in slope that defines the anomalies associated with both granites at or very close to 0 G.U. (0 mGal). This indicates that the regional field for the purpose of modelling the sub-surface geometry of the granites is well defined. However, the residual gravity maps do show small positive features on the outer rims of the anomalies with amplitudes ranging from 1.5 to < 0.1 G.U. (0.15 to < 0.01 mGal). This low amplitude positive rim may be due to an underestimation of the longer wavelenth components of the anomalies associated with the granites and/or an artefact of the censoring and contouring procedure. Since it represents 1.5 to 0.1% of the residual gravity amplitude, the positive rim has a very minor effect on the first order results of the forward gravity modelling presented below. Note also that the positive rim feature is absent in the region between the Götemar and Uthammar granites and therefore will have minimal influence on the gravity modelling results for the Laxemar model area.

2.75 D forward modelling of selected profiles sampled from the residual gravity map was performed using the Geosoft program GM-SYS. Although a wide range of possible density values and model shapes were evaluated, those presented here are considered to be the most successful based on fit to the observed residual anomalies and geological and petrophysical contraints.

A density value of 2,590 kg/m^3 was chosen for both the Götemar and Uthammar granites (cf. values of 2,600 and 2,590 kg/m^3 used for modelling of Bouguer gravity anomalies by /Triumf 2004/). Although this value is 10 to 30 kg/m^3 lower than petrophysical measurements by SGU, it is considered to be a representative density for the bulk of the intrusions, given the presence of aplites with density < 2,600 kg/m^3. A density value of 2,730 kg/m^3 was used to model the wall rocks of the intrusions. This value was estimated by taking the proportions of lithologies recorded in boreholes KLX06 and KLX02, and applying a linear mixing model using the density values for rock types reported at Laxemar by /Mattsson et al. 2004/. Given the variance in the petrophysical data, these calculations give bulk densities of 2,700 to 2,730 kg/ m^3 for KLX06 and 2,720 to 2,750 kg/m^3 for KLX02. Note that if a higher density value is used for the Götemar and Uthammar granites (e.g. 2,620 kg/m^3) then the wall rock density should be increased accordingly in order to maintain an acceptable fit between observed and modelled residual gravity profiles.

Four model profiles are presented here (Figure 3-7 to Figure 3-14). P1 crosses both the Götemar and Uthammar granites and the intervening Laxemar model area (Figure 3-6). P2 and P3 are EW and NS profiles over the Götemar granite, respectively. Boreholes KLX05, KLX06 and KLX09 have been projected into P3. P4 trends NNW-SSE and crosses the Götemar granite such that it also includes deep borehole KLX01.

In addition to constraining appropriate density differences for the gravity models a second geological control concerns the dip of the contacts of the intrusions at the surface, which is not currently known. This problem has been taken into account by defining two end-member geometrical models. In the "unconstrained" models presented below the near surface inclination of the contact is allowed to vary in order to achieve a best fit to the observed residual gravity anomalies. Conversely, in the "constrained" models the near surface contact is forced to conform to a vertical attitude, and the underlying structure is varied to determine the geometry that best fits the gravity observations. Available borehole information is used to evaluate the success of both the unconstrained and constrained gravity model results.

3.6 Gravity modelling results

In all model profiles the observed residual anomaly is plotted as solid circles and the gravity response of the model is a thin black curve. The red curve shows the RMS error of the model gravity to the observed gravity. Note that the units employed for modelling purposes are mGal.

3.6.1 P1: N-S Profile, Götemar and Uthammar granites and Laxemar model area

In the unconstrained gravity models of both intrusions (Figure 3-7), the upper contacts (roofs) dip outwards with moderate to shallow dips to depths of ~500 to ~1,000 m. Below this depth the lower contacts (floors) dip gently inwards to centrally located feeder zones that taper downward to depths of ~10 km (Götemar) and ~4 km (Uthammar). In these models, the upper contact of both the Götemar and Uthammar granite is predicted to dip beneath Laxemar, in agreement with previous modelling studies of the Bouguer gravity field /Triumf 2004, Nisca 1987/.

In the constrained gravity model (Figure 3-8) both plutons have vertical contacts to depths between ~500 m and 1,000 m, at which point the roofs dip gently outward to a depths of between 1,000 to 1,500 m. The floors of both plutons are generally flat, except for downward tapering root zone, which continue to depths of ~3 km.

Of note in both model types is that the residual gravity anomaly over the Laxemar model area can be almost fully accounted for by the gravity effects of the Götemar and Uthammar intrusions. This implies that previous gravity models that were designed to investigate the shorter wavelength contributions of individual rock units within the Laxemar model area /Triumf 2004/ may have underestimated the gravity effects of the Götemar and Uthammar plutons.

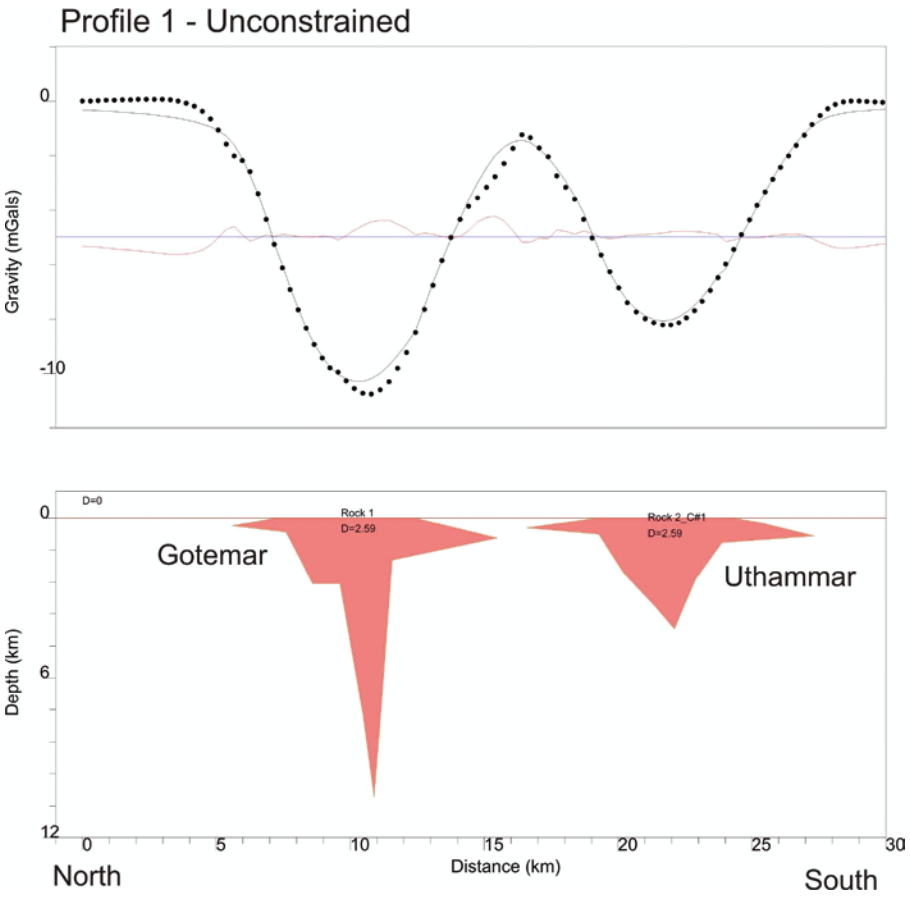

Figure 3-7. *North-south Profile P1 – unconstrained. Upper diagram plots observed (dotted) and modelled (solid black line) residual gravity profiles, and residual (RMS) error (red curve). Lower diagram shows modelled pluton geometry (pink polygons).*

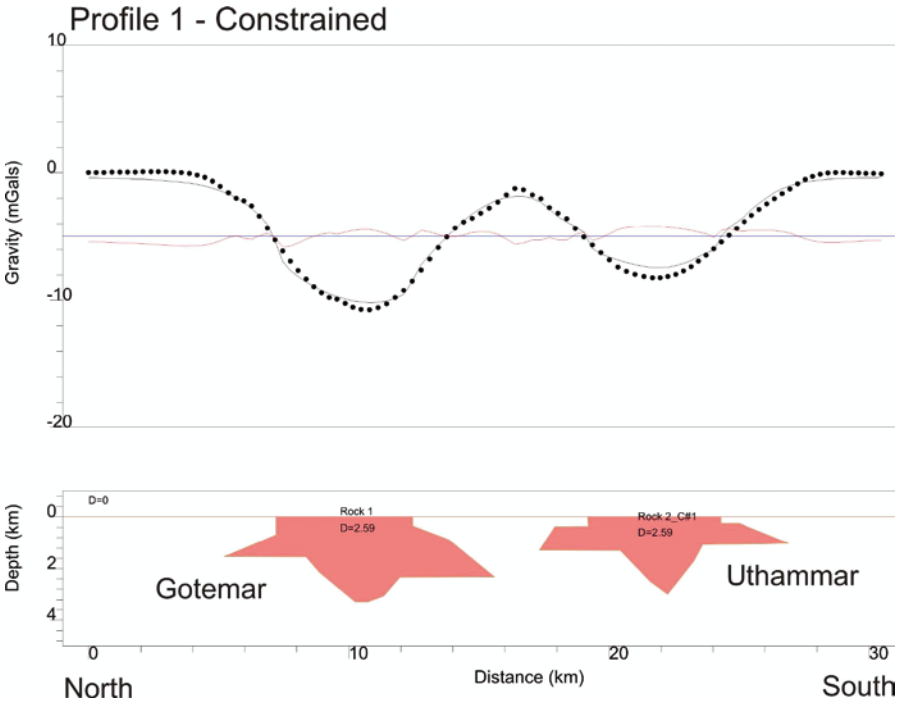

Figure 3-8. *North-south Profile P1 – constrained. See Figure 3-7 caption for further details.*

3.6.2 P2: Götemar granite E-W Profile

The E-W gravity profiles across the Götemar granite display similar first order geometry to P1. In the unconstrained model the western upper contact dips very gently outward to a shallow depth (< 100 m). However, this model solution does not achieve a reasonable fit with the outer flank of the residual anomaly (Figure 3-9). A good fit to the residual gravity low is obtained by a wide root zone extending to a depth of ~5 km. The constrained gravity model achieves superior fit to the observed residual gravity data (Figure 3-10). Vertical western and eastern contacts extend to depths of ~800 m and ~400 m, respectively, below which the roof dips moderately to steeply outward to meet a flat floor at ~2.5 km. A centrally located, downward tapering root extends down to ~3.8 km.

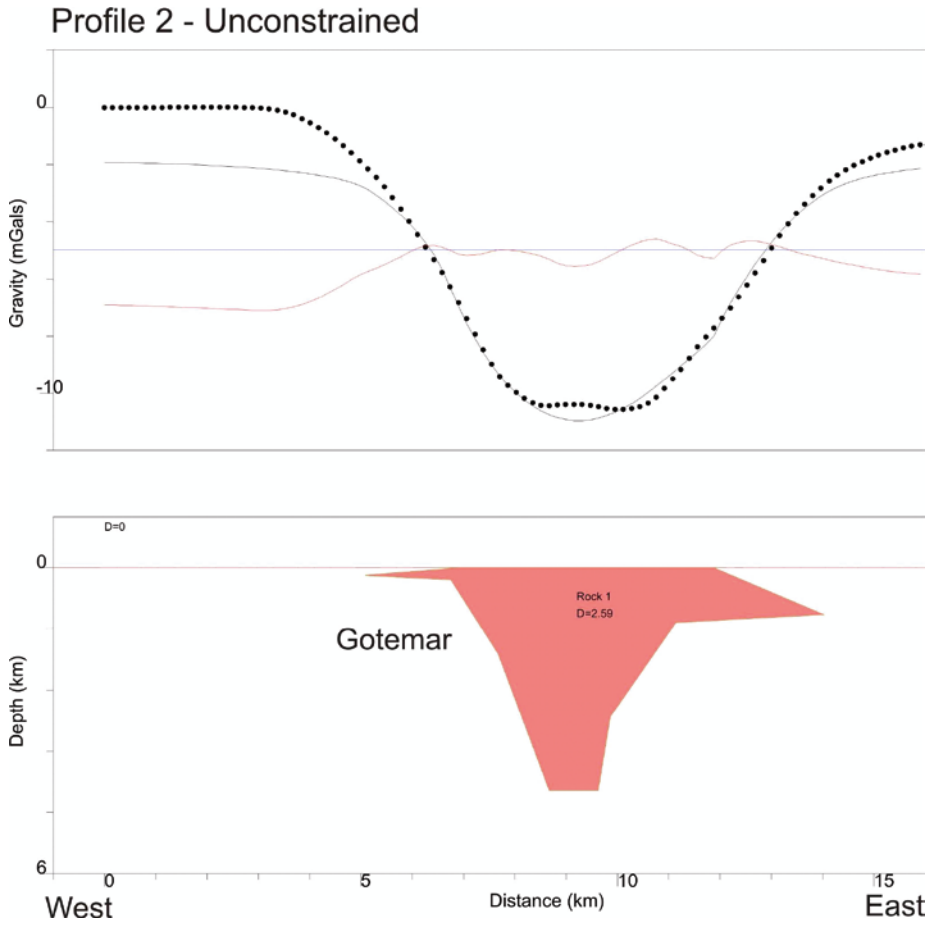

Figure 3-9. *Götemar W-E Profile P2 – unconstrained. See Figure 3-7 caption for further details.*

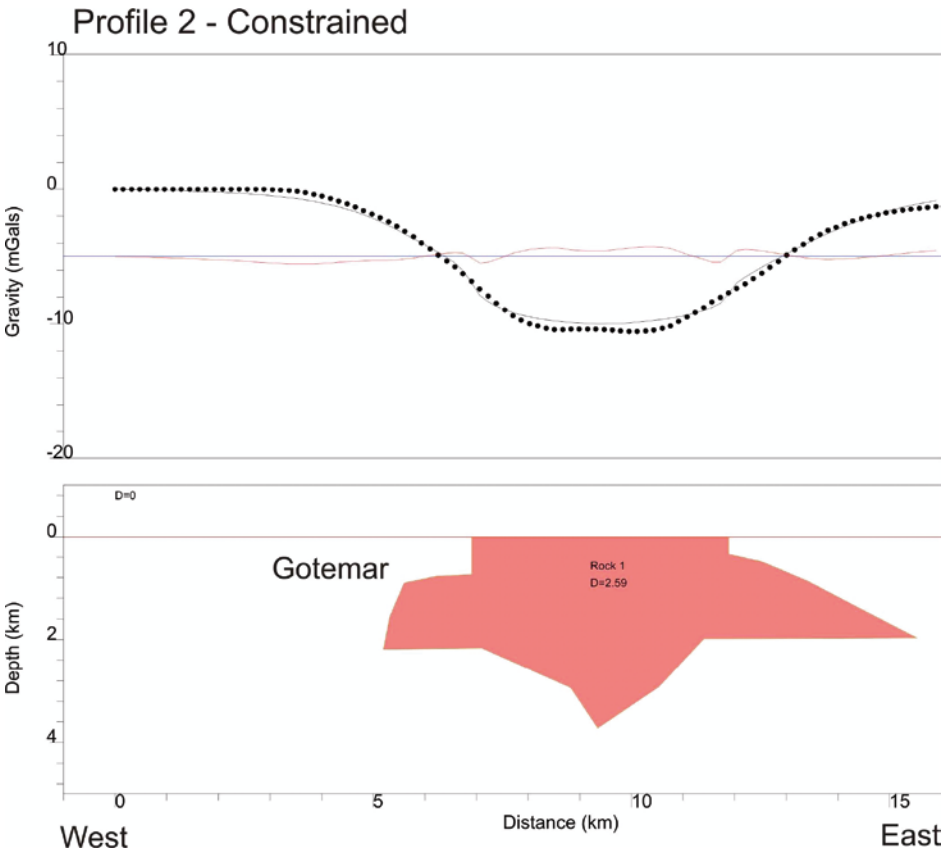

Figure 3-10. *Götemar W-E Profile P2 – constrained. See Figure 3-7 caption for further details.*

3.6.3 P3: Götemar granite N-S Profile

Both the unconstrained and constrained NS profiles are similar to those obtained in P1. In the unconstrained model the upper contact dips moderately to steeply outward to a depth of ~1,000 m (Figure 3-11). The floor dips gently inward to a downward tapering root that is ~6 km deep. In the constrained model vertical contacts at surface extend to depths of ~500 m (north) and 300 m (south), then dip moderately to gently outwards to a flat floor at ~2.5 km (Figure 3-12). A small root zone is predicted below the southern margin of the pluton.

Boreholes KLX06 and KLX09 project into the modelled Götemar granite in the unconstrained case (Figure 3-11). However, the same boreholes terminate above the roof of the Götemar granite in the constrained case (Figure 3-12). Since neither of these boreholes intersect the Götemar granite it can be concluded that the constrained model is a better fit to known subsurface data.

3.6.4 P4: Götemar granite NNW-SSE Profile

Profile P4 was selected to take advantage of deep borehole KLX01 as an additional control on the model results. Both the unconstrained and constrained profiles are similar to those for Profile 3. However, the unconstrained model (Figure 3-13) is clearly unacceptable because borehole KLX01 should pass through the SSE subsurface extension of the Götemar granite, which it does not. In the constrained model (Figure 3-14) borehole KLX01 terminates several hundred meters above the modelled SSE subsurface extension of the Götemar granite. As with Profile 3, the constrained model geometry is therefore a better fit to the available surface and subsurface geological data.

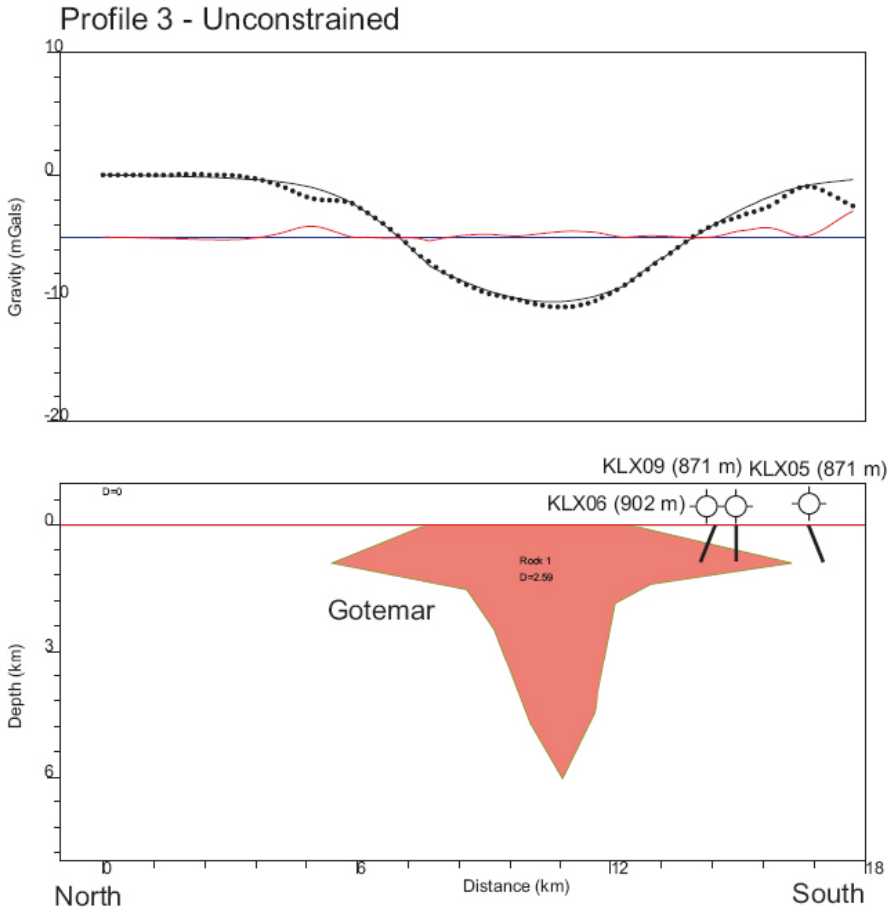

Figure 3-11. *Götemar N-S Profile P3 – unconstrained. See Figure 3-7 caption for further details. Borehole collars and traces are indicated.*

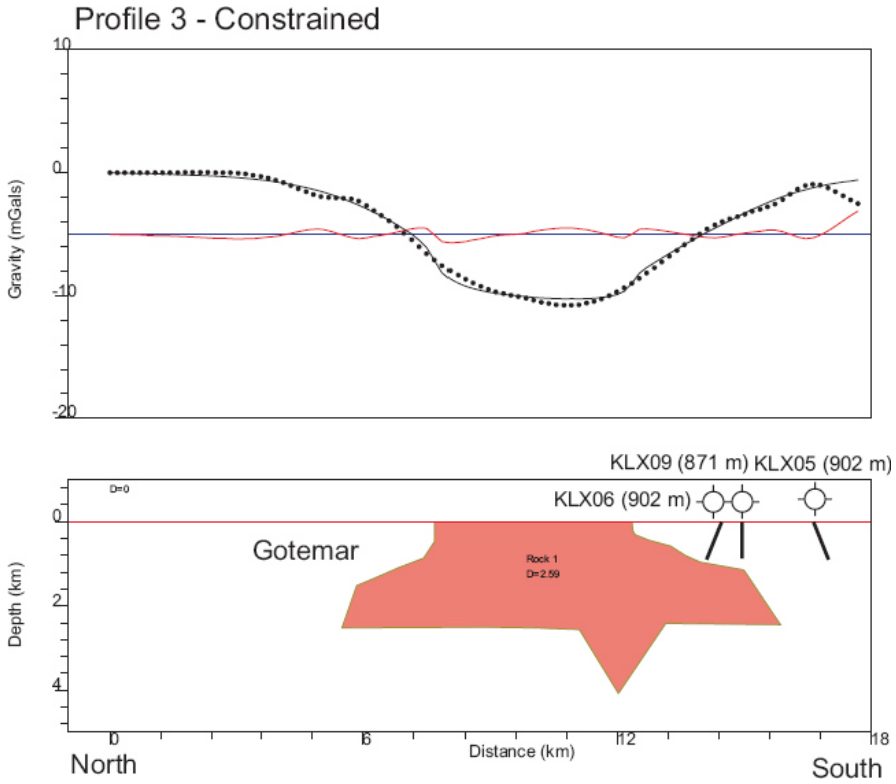

Figure 3-12. *Götemar N-S Profile P3 – constrained. See Figure 3-7 caption for further details. Borehole collars and traces are indicated.*

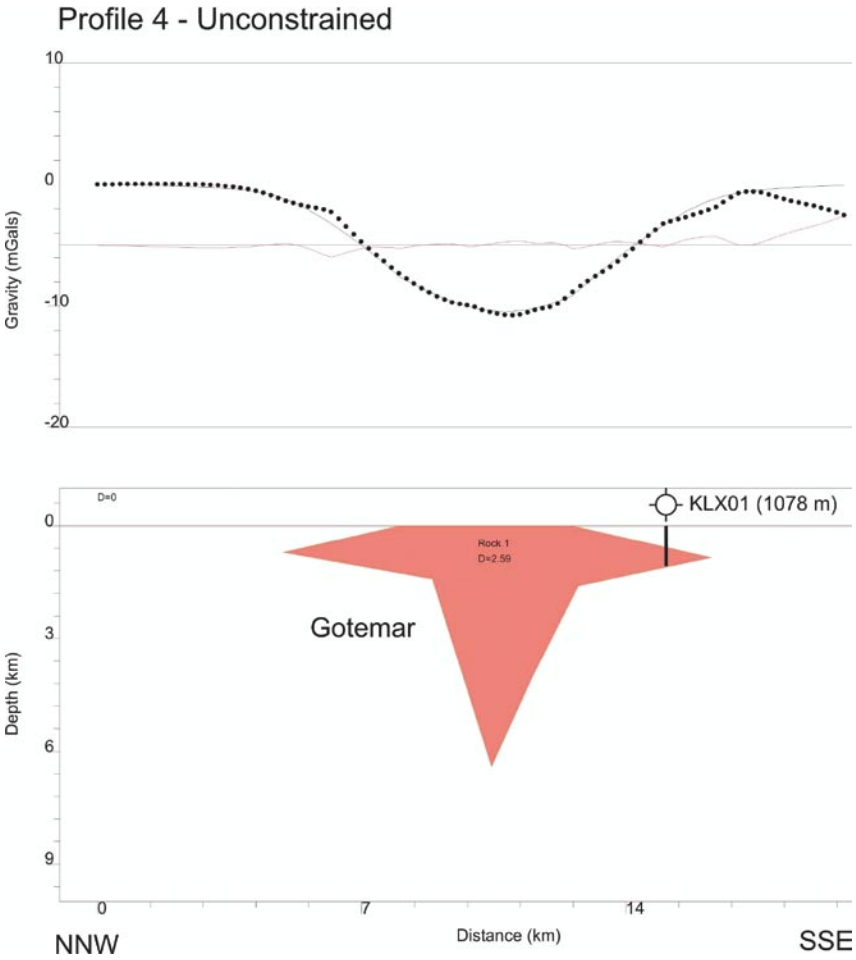

Figure 3-13. *Götemar NNW-SSE Profile P4 – unconstrained. See Figure 3-7 caption for further details. KLX01 borehole collars and trace are indicated.*

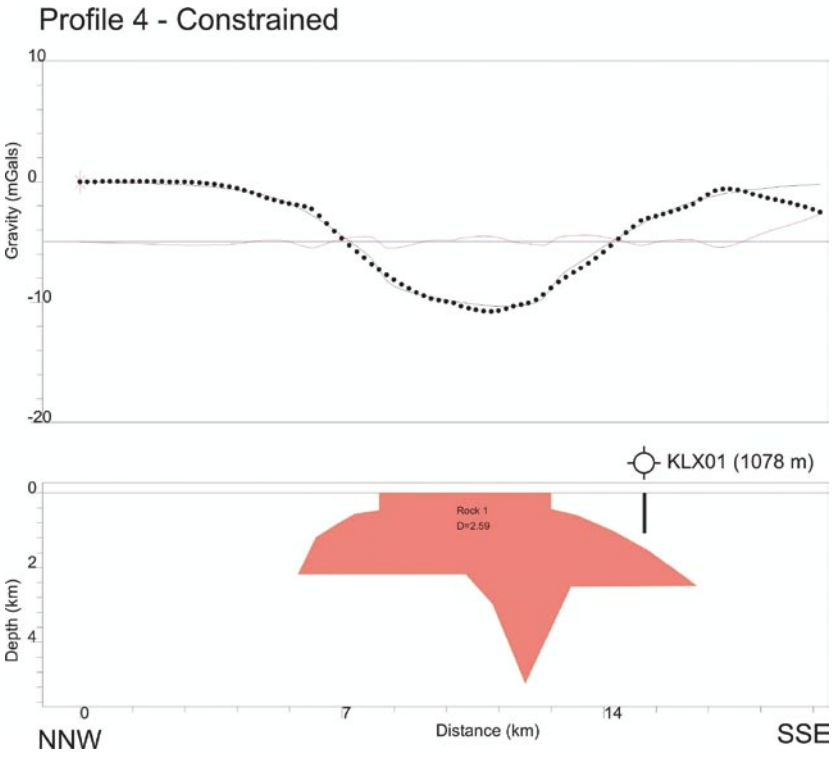

Figure 3-14. *Götemar NNW-SSE Profile P4 – constrained. See Figure 3-7 caption for further details. KLX01 borehole collars and trace are indicated.*

4 Discussion

4.1 Emplacement mechanism

Available geological and thermal data indicate that the Götemar and Uthammar granites were emplaced at shallow crustal depth into brittle wall rocks. Gravity modelling shows that both plutons have tabular to wedge shapes that are consistent with geophysical and field-based studies of granitic intrusions globally /e.g. Cruden 2006/. The dimensions of the Götemar and Uthammar granites (width and thickness) compare favourably with other felsic intrusions, falling at the low width end for plutons and the high thickness end for laccoliths on a logT vs. logL plot (Figure 2-4). The gravity model geometries are indicative of two possible emplacement mechanisms. The unconstrained gravity models are characterised by sill-like bodies of low aspect ratio with gently curved convex upward and downward roofs and floors, respectively, underlain by a narrow root zone. The geometry of the constrained gravity models resembles closely that of "punched laccoliths" /Corry 1988/. Punched laccoliths are characterised by flat floors, a domed roof and a faulted upper roof section (Figure 4-1). Emplacement mechanisms and the development of root zone structures are discussed in more detail below.

Sill formation involves a transition from vertical magma transport via a dyke or mobile hydrofacture to the propagation of a horizontal magma filled crack (Figure 4-1). Such transitions are thought to occur when a vertically propagating magma filled crack tip intersects a freely slipping fracture, a unit of high fracture toughness or a horizon of low ductility (Section 2). Outward propagation of the horizontal sill is governed by the wall rock fracture toughness, the available driving pressure and the magma viscosity. In an isotropic host medium the sill will spread out to form an outward tapering penny-shaped disk. Excess magma pressure and or emplacement of subsequent sills can lead to further elastic upward and downward bending of the sill roof and floor, respectively.

Further modification of the roof may occur by stoping and thermal fracturing to produce a dome-shaped geometry. Laccoliths may form if a vertically inflating sill is capable of interacting with the Earth's surface (Figure 2-5 and Figure 4-1). In this case the laccolith is characterised by a flat floor and bell-jar shaped, updomed roof that forms by elastic bending of the overlying strata (Figure 4-1a). If the roof curvature is large enough and elastic stresses in the overlying rocks exceed a critical value, the roof may fail to produce vertical faults that propagate to the Earth's surface. Once formed these faults allow further lifting of the roof due to excess magma pressure to form a punched laccolith (Figure 4-1c).

Neither the sill nor the laccolith emplacement mechanisms predict the formation of a substantial root zone, as determined for the Götemar and Uthammar granites. The geometry of the floors of both plutons suggests that downward displacement and rotation of the underlying crust has contributed to their vertical growth (e.g. the hybrid mechanisms in Figure 2-5). Floor depression has been proposed as an important space making mechanism for granite intrusions /Cruden 2006/. It is thought to be a result of mass exchange between a deflating magma source in the lower crust and an inflating pluton in the upper crust (Figure 2-6). Such downward displacement of the intervening crust can occur by both ductile and brittle deformation mechanisms and is consistent with the development of inward dipping floors and steeper sided root zones observed beneath many plutons.

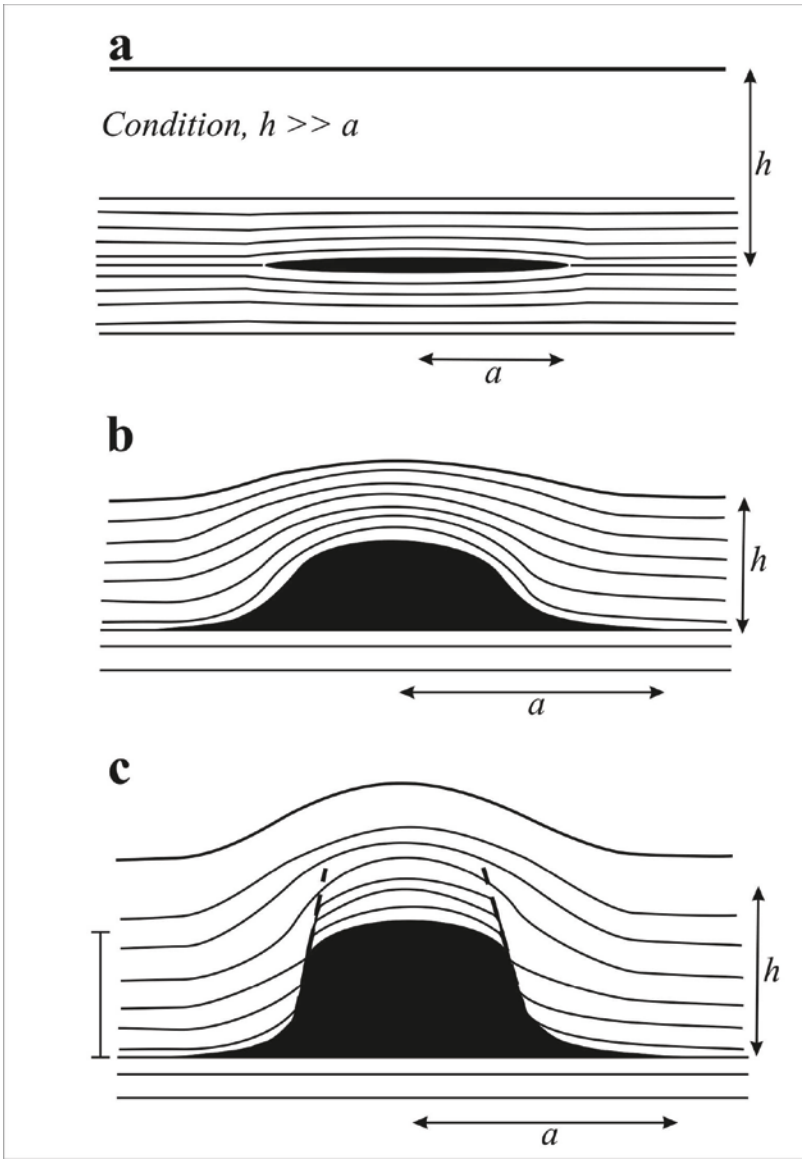

Figure 4-1. *Stages in the growth of a punched laccolith. (a) Initial sill propagation. (b) Vertical roof bending stage. (c) Roof failure stage.*

Constraints provided by boreholes coincident with gravity profiles suggests that a laccolith emplacement mechanism is most likely for the Götemar and Uthammar granites. Steep near surface contacts are also consistent with available aeromagnetic data (Triumf 2004, Sven Aaro, personal communication Nov. 2008). However, additional information on the dip of the contacts at the surface is required to fully resolve this question. This could be investigated by stripping of selected outcrops, shallow trenching, angled drilling, hammer seismic reflection profiling or detailed ground magnetic and gravity surveys. At this stage it can be concluded that both mechanisms are geologically feasible and consistent with current field observations and gravity modelling. Given the current constraints, the Götemar and Uthammar granites are best viewed as hybrid tabular intrusions whose space was created by components of both roof lifting and floor depression.

4.2 Implications for the structural development at Laxemar

The apparent conformity of ductile wall rock structures with the southern contact of the Götemar granite is not related to its emplacement. Rather, this structural pattern is inherited from a previous ductile deformation history related to the tectonics of the TIB at c. 1.80 Ga. Neither the Götemar nor the Uthammar granite are "diapirs" and their emplacement did not impose sufficient ductile strain on their wall rocks to be observed in the field. Although emplacement of both granites did not impose any observed ductile deformation on the wall rocks at the present level of exposure, the preferred laccolith emplacement model (Section 4.1) predicts that, at the present level of exposure, upward elastic bending of the roof and side rocks prior to roof failure was a likely consequence of the space-making process (Figure 4-1). Few systematic studies of fracture formation or reactivation due to laccolith roof bending are available for comparison, and none exist for laccolith emplacement into crystalline wall rocks. However, published field observations of sedimentary wall rocks of laccoliths /Johnson and Pollard 1973/ and well-known relationships between fold limbs and joints /Price and Cosgrove 1990/ suggest that new fractures may form in response to upward bending of wall rocks with orientations: 1) perpendicular to the intrusion margin (viz. *ac joints* associated with folds); 2) parallel to the intrusion margin (viz. *strike-parallel* or *bc joints* of folds); and 3) at high angles (> 70°) to the intrusion margin (viz. *cross-strike* or *hk0 joints* of folds) /Price and Cosgrove 1990/. If fractures with these orientations are present before emplacement, they are favourable candidates for reactivation.

Figure 4-2 identifies suitably oriented mapped lineaments that may correspond to fractures that were either reactivated or formed during emplacement of both granites. The criteria used to determine these fractures/lineaments were: 1) they occur in the regions located between the surface contacts of the granites and their subsurface lateral extents as determined by gravity modelling; 2) they have suitable orientations for fractures forming or reactivating during elastic bending of the plutons roofs, as discussed above; and 3) they do not cross-cut the intrusions. The latter criterion is somewhat problematic because a number of lineaments with regional trends (e.g. NW-SE in particular) that cross-cut the granites also make up a subset of the proposed emplacement-related structures. In this case, the lineaments either post-date intrusion or they are long-lived structures that were reactivated or formed before, during and after emplacement of the granites.

The outcrop pattern of the Uthammar granite is approximately rectilinear with contact orientations subparallel to mapped ENE- and NW-trending lineaments in the wall rocks (Figure 4-2). Emplacement of the circular Götemar granite likely formed or reactivated an array of suitably oriented fractures with contact sub-parallel and sub-perpendicular orientations (Figure 4-2). It should be noted that the proposed relationships between mapped fractures /Wahlgren et al. 2008/ and laccolithic emplacement of the Uthammar and Götemar granites is currently speculative and requires further testing. Such tests include: 1) detailed analysis of fractures with fracture fillings that are considered to be coeval with emplacement of the Uthammar and Götemar granites; 2) microstructural studies of the pluton wall rocks to test for the presence of stress-sensitive low-T microstructures; and 3) numerical and/or laboratory modelling to better understand and predict brittle, crystalline wall rock responses to laccolith emplacement. Carrying out these tests was beyond the scope of the present study.

Resetting of Ar-Ar systematics in biotite at c. 1.43 Ga is consistent with re-heating of wall rocks to above 300°C following emplacement of the Götemar and Uthammar granites. The subsurface lateral extent of both intrusions (Figure 4-2) and their volume as determined by gravity modelling explains why this re-heating event is observed at considerable distances from the surface contacts of the intrusions /Page et al. 2007, Söderlund et al. 2008/. Furthermore, some fracture filling mineral assemblages are interpreted to have been precipitated during emplacement the Götemar and Uthammar granites /Wahlgren et al. 2008/. This suggests that a transient hydrothermal system was established during the cooling and crystallization of the granites with the bulk of fluid flow and therefore heat loss occurring through the existing wall-rock fracture network.

The Götemar and Uthammar granites appear to be anorogenic intrusions, with no indications that upper crustal tectonic deformation participated in the emplacement and space-making process. However, preliminary interpretation of regional aeromagnetic data suggests that the granites occur within a broad NNE-SSW trending linear belt (Figure 3-2). Deep-seated tectonic control of both the lower crustal melting regime and the location of upper-crustal emplacement sites during the c. 1.4 Ga magmatic event is therefore likely.

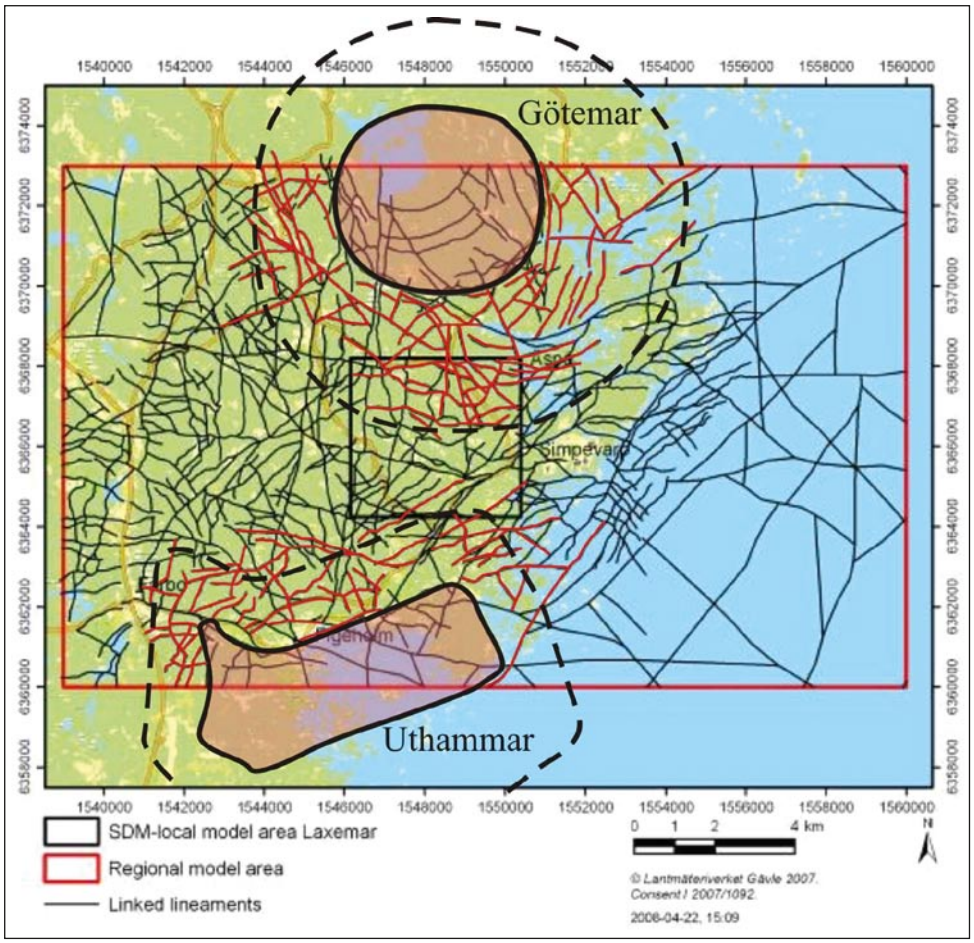

Figure 4-2. *Surface contacts (solid black contours) and subsurface lateral extents (dashed black contours), determined by gravity models, of the Götemar and Uthammar granites (semi-transpatent pink areas) superimposed on the linked lineament map for the Regional and SDM-local model areas /Wahlgren et al. 2008/. Red lines are mapped lineaments that may correspond to fractures that were reactivated of formed during emplacement of the Götemar and Uthammar granites at c. 1.45 Ga.*

5 References

Ablay G J, Clemens J D, Petford N, 2008. Large-scale mechanics of fracture-mediated felsic magma intrusion driven by hydraulic inflation and buoyancy pumping. In K Thompson and N Petford (eds) Structure and emplacement of high-level magmatic systems. Geological Society, London, Special Publications 302, in press.

Åhäll K-I, 2001. Åldersbestämning av svårdaterade bergarter i sydöstra Sverige. SKB R-01-60, Svensk Kärnbränslehantering AB.

Ameglio L, Vigneresse JL, 1999. Geophysical imaging of the shape of granitic intrusions at depth: a review. In A Castro, C Fernandez and J-L Vigneresse (eds) Understanding Granites: Integrating New and Classical Techniques. Geological Society, London, Special Publications 168, 39–54.

Annen C, Blundy J D, Sparks R S J, 2006. The genesis of intermediate and silicic magmas in deep crustal hot zones. Journal of Petrology 47, 505–539.

Bateman R, 1984. On the role of diapirism in the segregation, ascent and final emplacement of granitoid magmas. Tectonophysics 110, 211–231.

Benn K, Odonne F, Saint Blanquat M, 1998. Pluton emplacement during transpression in brittle crust: new views from analogue experiments. Geology 26, 1079–1082.

Benn K, Roest W R, Rochette P, Evans N G, Pignotta G S, 1999. Geophysical and structural signatures of syntectonic batholith construction: the South Mountain Batholith, Meguma Terrane, Nova Scotia. Geophysical Journal International 136, 144–158.

Björk L, 1986. Beskrivning till bergrundskartan Filipstad NV (with English Summary). Sveriges Geologiska Undersökning Af147.

Bouchez J-L, 1997. Granite is never isotropic: an introduction to AMS studies of granitic rocks. In Bouchez J-L, Hutton D H W, and Stephens W (eds) Granite: From Segregation of Melt to Emplacement Fabrics, Kluwer Academic Publishers, Dordrecht, pp. 95–112.

Bott M H P, and Smithson S B, 1967. Gravity investigations of subsurface shape and mass distributions of granite batholiths. Geological Society of America Bulletin 78, 859–878.

Branch C D, 1967. The source of eruption for pyroclastic flows: caldrons or calderas? Bulletin of Volcanology 30, 41–53.

Bridgwater D, Sutton J, and Watterson J, 1974. Crustal downfolding associated with igneous activity. Tectonophysics 21, 57–77.

Brisbin W C, 1986. Mechanics of pegmatite intrusion. American Mineralogist 71, 644–651.

Brown E H, and McClelland W C, 2000. Pluton emplacement by sheeting and vertical ballooning in part of the southeast Coast Plutonic Complex, British Columbia. Geological Society of America Bulletin 112, 708–719.

Brown E H, and Walker N W, 1993. A magma loading model for Barrovian metamorphism in the southeast Coast Plutonic Complex, British Columbia and Washington. Geological Society of America Bulletin 105, 479–500.

Brown M, 2001. Crustal melting and granite magmatism: key issues. Physics and Chemistry of the Earth 26, 201–212.

Brown M, 1994. The generation, segregation, ascent and emplacement of granite magma: the migmatite-to-crustally-derived granite connection in thickened orogens. Earth Science Reviews 36, 83–130.

Brown M, Solar G S, 1998. Granite ascent and emplacement during contractional deformation in convergent orogens. Journal of Structural Geology 20, 1365–1393.

Brun J P, Pons J, 1981. Strain patterns of pluton emplacement in a crust undergoing non-coaxial deformation, Sierra Morena, S. Spain. Journal of Structural Geology 3, 219–229.

Brun J P, Gapais D, Cogne J P, 1990. The Flamanville granite (northwest France): an unequivocal example of a syntectonically expanding pluton. Geological Journal 25, 271–286.

Buddington A F, 1959. Granite emplacement with special reference to North America. Geological Society of America Bulletin 70, 671–747.

Bussell M A, Pitcher W S, Wilson P A, 1976. Ring complexes of the Peruvian Coastal Batholith: a long-standing subvolcanic regime. Canadian Journal of Earth Science 13, 1020–1030.

Castro A, 1986. Structural pattern and ascent model in the central Extramadura batholith, Hercynian belt, Spain. Journal of Structural Geology 8, 633–645.

Clark D B, Henry A S, White, M A, 1998. Exploding xenoliths and the absence of 'elephant's graveyards' in granite batholiths. Journal of Structural Geology 20, 1325–1343.

Clemens J D, Mawer C K, 1992. Granitic magma transport by fracture propagation. Tectonophysics 204, 339–360.

Clemens J D, Petford N, 1999. Granitic melt viscosity and silicic magma dynamics in contracting tectonic settings. Journal of the Geological Society London 156, 1057–1060.

Cloos H, 1923. Das batholithenproblem. Forschritte Geologie und Paleontologie 1, 1–80.

Clough C T, Maufe H B, Bailey E B, 1909. The cauldron-subsidence of Glen Coe, and the associated igneous phenomena. Journal of the Geological Society London 65, 611–678.

Cobbing E J, 1999. The Coastal Batholith and other aspects of Andean magmatism in Peru. In: Castro A., Fernandez C, Vigneresse J-L. (eds) Understanding Granites: Integrating New and Classical Techniques. Geological Society, London, Special Publications 168, 111–122.

Coleman D S, Gray W, Glazner A F, 2004. Rethinking the emplacement and evolution of zoned plutons: Geochronologic evidence for incremental assembly of the Tuolumne Intrusive Suite, California, Geology 32, 433–436.

Corry C E, 1988. Laccoliths: Mechanics of emplacement and growth. Geological Society of America, Special Publication 220, 110 pp.

Courrioux G, 1987. Oblique diapirism: the Criffel granodiorite/granite zoned pluton (southwest Scotland). Journal of Structural Geology 9, 87–103.

Cruden A R, 1986. Shear zone analysis in the Svecofennian south of Västervik: implications for the structure of SE Sweden. Abstract. 17th Nordic Geological Meeting, Helsinki.

Cruden A R, 1990. Flow and fabric development during the diapiric rise of magma. Journal of Geology 98, 681–698.

Cruden A R, 1998. On the emplacement of tabular granites. Journal of the Geological Society 155, 853–862.

Cruden A R, 2006. Emplacement and growth of plutons: implications for rates of melting and mass transfer in continental crust. In M Brown and T Rushmer (eds.) Evolution and Differentiation of the Continental Crust, Cambridge University Press, pp. 455–519.

Cruden A R, Aaro S, 1992. The Ljugaren granite massif, Dalarna, central Sweden. Geologiska Föreningens i Stockholm Förhandlingar 114, 209–225.

Cruden A R, Launeau P, 1994. Structure, magnetic fabric and emplacement of the Archean Lebel Stock, S.W. Abitibi Greenstone belt. Journal of Structural Geology 16, 677–691.

Cruden A R, McCaffrey K J W, 2001. Growth of plutons by floor subsidence: implications for rates of emplacement, intrusion spacing and melt-extraction mechanisms. Physics and Chemistry of the Earth, Part A, Solid Earth and Geodesy 26, 303–315.

Cruden A R, McCaffrey K J W, 2002. Different scaling laws for sills, laccoliths and plutons: Mechanical thresholds on roof lifting and floor depression. In Breitkreuz C, Mock A and Petford N (eds) First International Workshop: Physical Geology of Subvolcanic Systems – Laccoliths, Sills and Dykes (LASI). Wissenschaftliche Mitteilung Instute für Geologie Technische Universität Bergakademie Freiberg 20/2002, 15–17.

Cruden A R, Sjöström H, Aaro S, 1999a. Structure and geophysics of the Gåsborn granite, Central Sweden: an example of fracture-fed asymmetric pluton emplacement. In: Castro A, Fernandez C and Vigneresse J.L (Eds) Understanding Granites: Integrating New and Classical Techniques. Geological Society, London, Special Publications 168, 141–160.

Cruden A R, Tobisch O T, Launeau P, 1999b. Magnetic fabric evidence for conduit-fed emplacement of a tabular intrusions: Dinkey Creek Pluton, central Sierra Nevada batholith, California. Journal of Geophysical Research 104, 10, 511–10, 530.

Culshaw N, Bhatnagar P, 2001. The interplay of regional structure and emplacement mechanisms at the contact of the South Mountain Batholith, Nova Scotia: floor-down or wall-up? Canadian Journal of Earth Sciences 38, 1285–1299.

Dehls J D, Cruden A R, Vigneresse J-L, 1998. Fracture control of late-Archean pluton emplacement in the Northern Slave Province, Canada. Journal of Structural Geology 20, 1145–1154, 1998.

Dingwell D B, 1999. Granitic melt viscosities. In: Castro A, Fernandez C and Vigneresse J-L (Eds) Understanding Granites: Integrating New and Classical Techniques. Geological Society, London, Special Publications 168, 27–38.

Dixon J M, Simpson D G, 1987. Centrifuge modelling of laccolith intrusion. Journal of Structural Geology 9, 87–103.

Evans D J, Rowley W J, Chadwick R A, Kimbell G S, Millward D, 1994. Seismic reflection data and the internal structure of the Lake District batholith, Cumbria, northern England. Proceedings of the Yorkshire Geological Society 50, 11–24.

Everitt R, Brown A, Ejeckam R, Sikorsky R, Woodcock D, 1998. Litho-structural layering within the Archean Lac du Bonnet Batholith, at AECL's Underground Research Laboratory, Southeastern Manitoba. Journal of Structural Geology 20, 1291–1304.

Fowler T K Jr, Paterson S R, 1997. Timing and nature of magmatic fabrics from structural relations around stoped blocks. Journal of Structural Geology 19, 209–224.

Glazner A F, Miller D M, 1997. Late-stage sinking of plutons. Geology 25, 1099–1102.

Glazner A F, Bartley J M, Coleman D S, Gray W, Taylor R Z, 2004. Are plutons assembled over millions of years by amalgamation from small magma chambers? GSA Today 14, 4–11.

Grocott J, Garde A, Chadwick B, Cruden A R, Swager C, 1999. Emplacement of Rapakivi granite and syenite by floor depression and roof uplift in the Paleoproterozoic Ketilidian orogen, South Greenland. Journal of the Geological Society, London 156, 15–24.

Guillot S, Pecher A, Rochette P, Le Fort P, 1993. The emplacement of the Manaslu granite of central Nepal: field and magnetic susceptibility constraints. In Treloar P J and Searle M P (eds) Himalayan Tectonics, Geological Society Special Publication 74, 413–428.

Hamilton W, 1988. Tectonic setting and variations with depth of some Cretaceous and Cenozoic structural and magmatic systems of the Western United States. In: Ernst W.G. (Ed) Metamorphism and Crustal Evolution of the Western United States: Rubey Volume 7. Prentice Hall, New Jersey, p. 1–40.

Hamilton W, Myers W B, 1967. The nature of batholiths. United States Geological Survey Professional Paper 554(c), 1–30.

Hamilton W, Myers W B, 1974. Nature of the Boulder batholith of Montana. Geological Society of America Bulletin 85, 365–378.

Hecht L, Vigneresse J-L, 1999. A multidisciplinary approach combining geochemical, gravity and structural data: implications for pluton emplacement and zonation. In Castro A, Fernandez C and Vigneresse J-L (eds) Understanding Granites: Integrating New and Classical Techniques. Geological Society, London, Special Publications 168, 95–110.

Hogan J P, Gilbert M C, 1995. The A-type Mount Scott granite sheet: importance of crustal magma traps. Journal of Geophysical Research 100, 15779–15792.

Hogan J P, Price J D, Gilbert M C, 1998. Magma traps driving pressure: consequences for pluton shape and emplacement in an extensional regime. Journal of Structural Geology 20, 1155–1168.

Holder M T, 1979. An emplacement mechanism for post-tectonic granite and its implication for geochemical features. In: Atherton M and Tarney J (eds.) Origin of Granite and Batholiths: Geochemical Evidence, Shiva, Kent, pp. 116–128.

Hunt C B, Averitt P, Miller R L, 1953. Geology and geography of the Henry Mountains region, Utah. U. S. Geological Survey Professional Paper 228, 234p.

Hutton D H W, Brown P E, 2000. Discussion of: Emplacement of Rapakivi granite and syenite by floor depression and roof uplift in the Paleoproterozoic Ketilidian orogen, South Greenland Journal of the Geological Society, London 157, 701–704.

Hutton D H W, Dempster T J, Brown P E, Becker S M, 1990. A new mechanism of granite emplacement: intrusion into active extensional shear zones. Nature 343, 452–455.

Jackson M D, Pollard D D, 1988. The laccolith-stock controversy: new results from the southern Henry Mountains, Utah. Geological Society of America Bulletin 100, 117–139.

Johnson A M, Pollard D D, 1973. Mechanics of growth of some laccolithic intrusions in the Henry Mountains, Utah, I. Field observations, Gilbert's model, physical properties and flow of the magma. Tectonophysics 18, 261–309.

John B E, Mukasa, S B, 1990. Footwall rocks of the Mid-Tertiary Chemehuevi detachment fault: a window into the middle crust in the Southern Cordillera. Journal of Geophysical Research 95, 463–485.

Kresten P, Chyssler J, 1976. The Götemar massif in south-eastern Sweden: A reconnaissance survey. Geologiska Föreningens i Stockholm Förhandlingar 98, 155–161.

Leake B E, Cobbing J, 1993. Transient and long-term correspondence of erosion level and the tops of granite plutons. Scottish Journal of Geology 29, 177–182.

Le Fort P, 1981. Manaslu leucogranite: a collision signature of the Himalaya a model for its genesis and emplacement. Journal of Geophysical Research 86, 10545–10568.

Leitch A M, Weinberg R F, 2002. Modelling granite migration by mesoscale pervasive flow. Earth and Planetary Science Letters 200, 131–146.

Lipman P W, 1984. The roots of ash flow calderas in western North America: windows into the tops of granitic batholiths. Journal of Geophysical Research 89, 8801–8841.

Lundberg E, Sjöström H, 2006. Oskarshamn site investigation. Kinematic analysis of ductile and brittle/ductile shear zones in Simpevarp and Laxemar subarea. SKB P-06-118, Svensk Kärnbränslehantering AB.

Lynn H B, Hale L D, Thompson G A, 1981. Seismic reflections from the basal contacts of batholiths. Journal of Geophysical Research 86, 10633–10638.

Mahon K I, Harrison T M, Drew D A, 1988. Ascent of a granitoid diapir in a temperature varying medium. Journal of Geophysical Research 93, 1174–1188.

Marsh B D, 1982. On the mechanics of igneous diapirism, stoping and zone melting. American Journal of Science 282, 808–855.

Marsh B D, 1984. Mechanics and energetics of magma formation and ascension. In Boyd F R Jr. (Ed) Explosive Volcanism: Inception, Evolution and Hazards. National Academy Press, Washington, p. 67–83.

Mattsson H, Thunehed H, Triumf C-A, 2004. Compilation of petrophysical data from rock samples and in situ gamma-ray spectrometry measurements. Stage 2 – 2004 (including 2002). SKB P-04-294, Svensk Kärnbränslehantering AB.

McCaffrey K J W, 1992. Igneous emplacement in a transpressive shear zone: Ox Mountains igneous complex. Journal of the Geological Society 149, 221–235.

McCaffrey K J W, Cruden A R. 2002. Dimensional data and growth models for intrusions. In Breitkreuz C, Mock A and Petford N (eds.) First International Workshop: Physical Geology of Subvolcanic Systems – Laccoliths, Sills and Dykes (LASI), Wissenschaftliche Mitteilungen der Bergakademie Freiberg 20, 37–39.

McCaffrey K J W, Petford N, 1997. Are granitic intrusions scale invariant? Journal of the Geological Society London 154, 1–4.

Mickus K L, Aiken C L V, Kennedy W D, 1991. Regional-residual gravity anomaly separation using the minimum-curvature technique. Geophysics 56, 279–283.

Miller C F, Wooden J L, Bennett V C, Wright J E, Solomon G C Hurst R W, 1990. Petrogenesis of the composite peraluminous-metaluminous Old Woman-Piute range batholith, southeastern California; isotopic constraints. Geological Society of America Memoir 174, 99–109.

Miller R B, Paterson S R, 1999. In defence of magmatic diapirs. Journal of Structural Geology 21, 1161–1173.

Molyneux S J, Hutton D H W, 2000. Evidence for significant granite space creation by the ballooning mechanism: the example of the Ardara pluton, Ireland. Geological Society of America Bulletin 112, 1543–1558.

Morgan S S, Law R D, Saint Blanquat M, 2000. Papoose Flat, Eureka Valley-Josua Flat-Beer Creek, and Sage Hen Flat plutons: examples of rising, sinking, and cookie cutter plutons in the central White-Inyo Range, eastern California. In: Lageson DR, Peters S G Lahren M M (Eds) Great Basin and Sierra Nevada: Boulder, Colorado, Geological Society of America Field Guide 2, p 189–204.

Myers J S, 1975. Cauldron subsidence and fluidization: mechanisms of intrusion of the Coastal Batholith of Peru into its own volcanic ejecta. Geological Society of America Bulletin 86, 1209–1220.

Nédélec A, Paquette J-L, Bouchez J-L, Olivier P Ralison B, 1994. Stratoid granites of Madagascar: structure and position in the Panafrican orogeny. Geodynamica Acta 7, 48–56.

Nisca D, 1987. Aerogeophysical interpretation bedrock and tectonic analysis. SKB HRL Progress Report 25-87-04, Svensk Kärnbränslehantering AB.

Nitescu B, Cruden A R, Bailey R C, 2003. Topography of the crust-mantle interface under the Western Superior craton from gravity modelling. Canadian Journal of Earth Science 40, 1307–1320.

Nylund B, 1987. Regional gravity survey of the Simpevarp area. SKB HRL Progress Report PR 25-87-20, Svensk Kärnbränslehantering AB.

Oliver H W, 1977. Gravity and Magnetic investigations of the Sierra Nevada batholith, California. Geological Society of America Bulletin 88, 445–461.

Page L, Söderlund P, Wahlgren C-H, 2007. Oskarshamn site investigation. $^{40}Ar/^{39}Ar$ and (U-Th)/He geochronology of samples from the cored boreholes KSH03A, KSH03B, KLX01, KLX02 and the access tunnel to the Äspö Hard Rock Laboratory. SKB P-07-160, Svensk Kärnbränslehantering AB.

Paterson S R, Fowler T K Jr, 1993. Re-examining pluton emplacement processes. Journal of Structural Geology 15, 191–206.

Paterson S R, Miller R B, 1998. Mid-crustal magmatic sheets in the Cascades Mountains, Washington: implications for magma ascent. Journal of Structural Geology 20, 1345–1363.

Paterson S R, Schmidt K L, 1999. Is there a close spatial relationship between faults and plutons? Journal of Structural Geology 21, 1131–1142.

Paterson S R, Tobisch O T, 1992. Rates of processes in magmatic arcs: implications for the timing and nature of pluton emplacement and wall rock deformation. Journal of Structural Geology 14, 291–300.

Paterson S R, Fowler T K Jr, Miller R B, 1996. Pluton emplacement in arcs: a crustal-scale exchange process. Transactions of the Royal Society of Edinburgh: Earth Sciences 87, 115–123.

Paterson S R, Vernon R H, Fowler T K Jr, 1991. Aureole tectonics. In Kerrick D M (Ed) Contact Metamorphism, Reviews in Mineralogy 26, 673–722.

Petford N, 1996. Dykes or diapirs? Transactions of the Royal Society of Edinburgh: Earth Sciences 87, 105–114.

Petford N, Kerr R C, Lister J R, 1993. Dike transport of granitoid magmas. Geology 21, 845–848.

Petford N, Cruden A R, McCaffrey K J W, Vigneresse J-L, 2000. Dynamics of granitic magma formation, transport and emplacement in the Earth's crust. Nature 408, 669–673.

Pitcher W S, 1993. The nature and origin of granite. Chapman and Hall, London, 321p.

Pitcher W S, 1979. The nature, ascent and emplacement of granitic magmas. Journal of the Geological Society, London 136, 627–662.

Pollard D D, Johnson A M, 1973. Mechanics of growth of some laccolithic intrusions in the Henry Mountains, Utah, II. Bending and failure of overburden layers and sill formation. Tectonophysics 18, 311–354.

Potter M E, Paterson S R, 2000. Rolling-hinge model for downward flow of host rock during emplacement of the Pachalka pluton, Mojave desert, southeastern California. Geological Society of America Abstracts with Programs 32, abstract 52968.

Price N J, Cosgrove J W, 1990. Analysis of geological structures. Cambridge University Press, Cambridge, UK, 516 pp.

Ramsay J G, 1989. Emplacement kinematics of a granite diapir: the Chinamora batholith, Zimbabwe. Journal of Structural Geology 11, 191–209.

Robin P-Y F, Cruden A R, 1994. Strain and vorticity patterns in ideally ductile transpression zones. Journal of Structural Geology 16, 447–466.

Rocchi S, Westerman D S, Dini A, Innocenti F, Tonarini S, 2002. Two-stage growth of laccoliths at Elba Island, Italy. Geology 30, 983–986.

Roman-Berdiel T, Gapais D, Brun JP, 1995. Analogue models of laccolith formation. Journal of Structural Geology 17, 1337–1346.

Rosenberg C L, Berger A, Schmid S M, 1995. Observations from the floor of a granitoid pluton: inferences on the driving force of final emplacement. Geology 23, 443–446.

Roy B, Clowes R M, 2000. Seismic and potential field imaging of the Guichon Creek batholith, British Columbia, Canada, to delineate structures hosting porphyry copper deposits. Geophysics 65, 1418–1434.

Rubin A M, 1993. Dykes vs. diapirs in viscoelastic rock. Earth and Planetary Science Letters 119, 641–659.

Saint Blanquat M, Law R D, Bouchez J-L, Morgan S S, 2001. Internal structure and emplacement of the Papoose Flat pluton: an integrated structural, petrographic, and magnetic susceptibility study. Geological Society of America Bulletin 113, 976–995.

Scaillet B, Pêcher A, Rochette P, Champenois M, 1995. The Gangotri granite (Garhwal Himalaya): Laccolithic emplacement in an extending collisional belt. Journal of Geophysical Research 100, 585–607.

Schmeling H, Cruden A R, Marquart G, 1988. Finite deformation in and around a fluid sphere moving through a viscous medium: implications for diapiric ascent. Tectonophysics,149, 17–34.

Searle M P, Metcalf R P, Rex A J, Norry M J, 1993. Field relations, petrogenesis and emplacement of the Bhangirathi leucogranite, Garhwal Himalaya. In Treloar P J and Searle M P (Eds) Himalayan Tectonics, Geological Society Special Publication 74, 429–444.

Skarmeta J J, Castelli J C, 1997. Intrusión sintectónica del granito de las Torres del Paine, Andes Patagónicos de Chile. Revista Geologica de Chile 24, 55–74.

Söderlund P, Page L, Söderlund U, 2008. $^{40}Ar/^{39}Ar$ biotite and hornblende geochronology from the Oskarshamn area, SE Sweden: Discerning multiple Proterozoic tectonothermal events. Geological Magazine 145, 190–799

Stephenson C T E, Owens W H, Hutton D H W, 2007a. Flow lobes in granite; the determination of magma flow direction in the Trawenagh Bay Granite, northwestern Ireland, using anisotropy of magnetic susceptibility. Geological Society of America Bulletin 119, 1368–1386.

Stephenson C T E, Owens W H, Hutton D H W, Hood D N, Meighan I G, 2007b. Laccolithic, as opposed to cauldron subsidence, emplacement of the Eastern Mourne Pluton, N. Ireland; evidence from anisotropy of magnetic susceptibility. Journal of the Geological Society, London 164, 99–110.

Sweeney J F, 1976. Subsurface distribution of granitic rocks, south-central Maine. Geological Society of America Bulletin 87, 241–249.

Sylvester A G, 1964. The Precambrian rocks of the Telemark area in south central Norway, III, geology of the Vrådal granite, Norsk Geologisk Tidsskrift 44, 445–482.

Talbot C J, Grantham G H, 1987. The Proterozoic intrusion and deformation of deep crustal 'sills' along the south coast of Natal. South African Journal of Geology 90, 520–538.

Taylor G K, 2007. Pluton shapes in the Cornubian Batholith; new perspectives from gravity modelling. Journal of the Geological Society, London 164, 525–528.

Tobisch O T, Fiske R S, Sorenson S S, Saleeby J B, Holt E, 2001. Steep tilting of metavolcanic rocks by multiple mechanisms, central Sierra Nevada, California. Geological Society of America Bulletin 112, 1043–1058.

Triumf C-A, 2004. Gravity measurements in the Laxemar model area with surroundings. SKB P-04-128, Svensk Kärnbränslehantering AB.

Vigneresse J-L, 1995. Control of granite emplacement by regional deformation. Tectonophysics 249, 173–186.

Vigneresse J-L, Bouchez J-L, 1997. Successive granitic magma batches during pluton emplacement: the case of Cabeza de Araya (Spain). Journal of Petrology 38, 1767–1776.

Vigneresse J-L, Tikoff B, Ameglio L, 1999. Modification of the regional stress field by magma intrusion and formation of tabular granitic plutons. Tectonophysics 302, 203–224.

Wahlgren, C-H, Hermanson J, Curtis P, Triumf C-A, Drake H, Tullborg E-L, 2006. Geological description of rock domains and deformation zones in the Simpevarp and Laxemar subareas. Preliminary site description Laxemar subarea – version 1.2. SKB R-05-69, Svensk Kärnbränslehantering AB.

Wahlgren C-H, Curtis P, Hermanson J, Forssberg O, Öhman J, Drake H, Fox A, La Pointe P, Triumf C-A, Mattsson H, Thunehed H, 2008. Geology Laxemar. Site descriptive modelling, SDM-Site Laxemar. SKB R-08-54, Svensk Kärnbränslehantering AB.

Weertman J, 1971. Theory of water-filled crevasses in glaciers applied to vertical magma transport beneath ocean ridges. Journal of Geophysical Research 76, 1171–1183.

Weinberg R F, Podlachikov Y, 1994. Diapiric ascent of magmas through power law crust and mantle. Journal of Geophysical Research, 99, 9543–9559.

Weinberg R F, Searle M P, 1998. The Pangong injection complex, Indian Karakoram: a case of pervasive granite flow through hot viscous crust. Journal of the Geological Society, London 155, 883–891.

Whitney J A, Stormer J C Jr, 1986. Model for the intrusion of batholiths associated with the eruption of large-volume ash-flow tuffs. Science 231, 483–485.

Wiebe R A, Collins W J, 1998. Depositional features and stratigraphic sections in granitic plutons: implications for the emplacement and crystallization of granitic magma. Journal of Structural Geology 20, 1273–1289.